Availability of particulate Fe to phytoplankton in the Sea of Okhotsk

Koji Sugie,[a*] Jun Nishioka,[b] Kenshi Kuma,[a, c] Yuri N. Volkov,[d] and Takeshi Nakatsuka[e]

a: Graduate School of Environmental Science, Hokkaido University, North 10, West 5, Kita-ku, Sapporo, Hokkaido 060-0810, Japan

b: Pan-Okhotsk Research Center, Institute of Low Temperature Science, Hokkaido University, North 19, West 8, Kita-ku, Sapporo, Hokkaido 060-0819, Japan

c: Faculty of Fisheries Science, Hokkaido University, 3-1-1 Minato-cho, Hakodate, Hokkaido 041-8611, Japan

d: Far Eastern Regional Hydrometeorological Research Institute, Vladivostok, Russia

e: Graduate School of Environmental Studies, Nagoya University, Furo-cho, Chikusaku, Nagoya, 464-8601, Japan

*: Author for corresponding:
Koji Sugie
Present address: Faculty of Environmental Earth Science, Hokkaido University, Kita 10 Nishi 5, Kita-ku, Sapporo, Hokkaido 060-0810, Japan.
E-mail: kojisugie@gmail.com
Tel & Fax: +81-11-706-2370

Key words: Iron; Particulate iron; Bioavailability; Diatom; Sea of Okhotsk; Nepheloid layer

- We investigated availability of particulate iron to marine phytoplankton.
- Suspended particulate matter (SPM) collected from the nepheloid layer was used.
- Iron in the SPM was available which provide healthy growth of phytoplankton.
- Such particulate iron supports biological production around the Kuril Islands.

ABSTRACT

In a shipboard incubation study, we investigated the availability of particulate iron (Fe) to an Fe-starved phytoplankton community through the addition of suspended particulate matter (SPM; > 1 μm) collected from the nepheloid layer in the coastal region of the Sea of Okhotsk. Surface seawater incubations were also conducted at three stations around the Bussol' Strait where the SPM that possibly originated from the coastal nepheloid layer could emerge to the surface mixed layer due to strong vertical mixing around the Kuril Islands. In the SPM-added experiment, the growth rate of phytoplankton was significantly enhanced by the addition of SPM compared to the unamended control. This result clearly indicates that Fe in the SPM collected from the nepheloid layer was available to marine phytoplankton. In addition, phytoplankton particularly coastal diatoms in the nepheloid layer were viable and showed healthy growth. In the surface seawater incubation experiments, phytoplankton growth and nutrient drawdown in unamended control conditions in two of the three stations may be supported by Fe from the particulate fraction (> 0.22 μm), as estimated from stoichiometric calculation. We suggest that the bioavailable particulate Fe in SPM of the coastal region supports biological production and nutrient drawdown even after the depletion of dissolved Fe around the Kuril Islands, where strong vertical mixing occurs.

1. Introduction

Iron (Fe) is the most important micronutrient for marine phytoplankton growth, because of its key role in processes such as photosynthesis and nitrate and nitrite assimilation (Raven et al., 1999). However, the thermodynamically stable oxidation state of Fe in oxic surface seawater is predominantly Fe(III), which has an extremely low solubility (Stumm and Morgan, 1996; Kuma et al., 1996). The Fe in the North Pacific Ocean is mainly derived from continental sources, such as eolian dust, riverine input, and sedimentary Fe from the continental shelf to coastal and oceanic waters (Johnson et al., 1999, 2005; Jickells et al., 2005; Lohan and Bruland, 2006; Nishioka et al., 2007). Moore and Braucher (2008) estimated the global-scale Fe cycle using the Biogeochemical Elemental Cycling ocean model and found that the sedimentary source of Fe contributes as much as 70% of dissolved Fe (D-Fe) in pools in the surface of the northwestern North Pacific. Previous studies indicated that the high Fe water mass possibly related to the sedimentary source would be transported from the western coast of the Sea of Okhotsk to the western North Pacific region via the Kurile Straits (Nishioka et al., 2007; Misumi et al., 2011).

In the Sea of Okhotsk, dense shelf water (DSW) is produced by brine rejection due to sea ice formation during winter, which originates in the region of the Siberian and Sakhalin continental shelves (Shcherbina et al., 2004; Matsuda et al., 2009). The DSW entrains continental sediments during the formation processes and is transported southward along the Sakhalin coast at an intermediate depth (~200–500-m), forming the Okhotsk Sea intermediate water (OSIW) (Fukamachi et al., 2004). Nakatsuka et al. (2004) reported that DSW has high particulate organic matter derived from coastal sediment, which should have high particulate Fe concentrations (e.g., Landing and Bruland, 1987; Elrod et al., 2008). The OSIW flows further southeastward and outflows into the western subarctic Pacific Ocean, through the Kurile Straits with strong vertical diapycnal mixing around the Kurile Islands (Nakamura and Awaji, 2004; Ito et al., 2010, 2011). The Bussol' Strait is a key channel with respect to the exchange of seawater between the Sea of Okhotsk and the Oyashio region (e.g., Yasuda et al., 2002) because the channel is deepest at the Kuril Straits. It can be assumed that the particles in the DSW advect into the surface of the Okhotsk and Oyashio waters via strong water mixing with the OSIW. Intrusion of such bio-active particles into the surface seawater would

affect and play an important role in phytoplankton communities around the region. However, little attention has been paid to the importance of particulate matter on the dynamics of surface phytoplankton communities.

In general, one of the most bioavailable Fe species for photolithoautotrophic phytoplankton is dissolved inorganic Fe (Fe′) (Anderson and Morel, 1982; Morel et al., 2008). There are apparent exceptions to this model in that organic Fe-ligand complexes could be indirectly and/or directly utilized by the cells (Hutchins et al., 1999a; Maldonado and Price, 2001; Shaked et al., 2005; Kustka et al., 2007). In nature, almost all of the dissolved Fe(III) should be bound to organic ligands, which have high and low binding affinities for Fe (Rue and Bruland, 1995). A recent study demonstrated that saccharides are responsible for binding Fe with low affinity in the colloidal size fraction (Hassler et al., 2011). The bioavailability of Fe-saccharide complexes is higher than for Fe binding with high-affinity ligands for eukaryotic phytoplankton (Hassler and Schoemann, 2009; Hassler et al., 2011). There is increasing evidence that the bioavailability of D-Fe should be different depending on the binding affinity of the ligand or differences in the phytoplankton groups and their habitats (Hutchins et al., 1999b; Kuma et al., 2000; Hassler and Schoemann, 2009; Strzepek et al., 2011).

The bioavailability of D-Fe species including the colloidal fraction (between < 200 kDa or 0.025 μm to 0.2 or 0.45 μm; e.g., Nishioka and Takeda, 2000; Nishioka et al., 2001) has been relatively well examined, although the availability of particulate Fe (P-Fe) is largely unknown. According to laboratory experiments (Kuma and Matsunaga, 1995; Yoshida et al., 2006), the surface reactivity or crystalline structure of solid inorganic Fe oxyhydroxide controls the supply of bioavailable D-Fe species for coastal diatoms. In natural conditions, Elrod et al. (2008) and Sugie et al. (2010a) reported that surface chlorophyll-*a* (Chl-*a*) concentrations have significant positive correlations with total dissolvable Fe concentrations (T-Fe), suggesting that particulate Fe supports a substantial portion of the ecosystem's Fe requirements. Using Chl-*a* and D- and P-Fe concentrations, Nakayama et al. (2010) calculated stoichiometrically that the phytoplankton biomass of intensive spring diatom blooms (> 10 μg Chl-*a* L^{-1}) in the Oyashio region of the western subarctic Pacific region can be achieved by the utilization of D-Fe and also Fe from the particulate phase. Furthermore, Fitzwater et al.

(2003) measured the T-Fe concentrations in the surface waters, which originated from the benthic boundary layer of the continental shelves during upwelling events that caused a substantial part of the Fe in the particulate fraction to be chemically labile (leachable by 25% acetic acid for 2 h). They also suggested that a small but substantial part of labile particulate Fe contributes to the bloom formation around the upwelling plumes (Fitzwater et al., 2003). Although those previous studies recognize the importance of particulate Fe as a source of bioavailable Fe, the availability of Fe in natural marine particles has not been examined before, except for Fe coming from aeolian dust (e.g., Payten et al., 2009).

In this study, we conducted two types of bioassay experiments to examine the availability of P-Fe for the growth of phytoplankton. First, we examined the availability of Fe associated with marine suspended particulate matters for an Oyashio phytoplankton community through the addition of particulate matters collected in the DSW (SPM_{DSW}). Second, surface phytoplankton communities at three stations around the Bussol' Strait were incubated to investigate the importance of P-Fe for the growth of phytoplankton where SPM_{DSW} could appear in the surface mixed layer. The availability of the P-Fe in the surface waters was evaluated by stoichiometric calculations using Chl-*a* concentration increases and nutrient drawdown data with reported Fe:C and Fe:Chl-*a* values. Our results provide the first direct evidence of the availability of Fe in marine suspended particulate matters for natural phytoplankton communities.

2. Methods

2.1. SPM_{DSW} addition experiment

Phytoplankton incubations were performed aboard the R/V Professor Khromov during August to September 2007 (Kh-07 cruise). Natural phytoplankton communities used in incubation experiments for the bioavailability of Fe in the SPM_{DSW} were collected in the Oyashio region (Stn Oy: 46°00'N 152°30'E; Fig. 1) using an acid-cleaned Teflon-coated 10 L Niskin X sampling bottle (General Oceanics) attached to a CTD-carousel multi-sampling system (Nishioka et al., 2007, 2011). Hydrographic data (salinity, temperature, and depth) and transmittance were obtained using a CTD (Sea-Bird, Model 9-puls) and transmissometers (Wet Labs, C-Star). Seawater for a natural phytoplankton stock was sieved with 100 μm

121 acid-cleaned Teflon-mesh to eliminate mesozooplankton and nutrients were added [27 μmol
122 L^{-1} NO_3, 2 μmol L^{-1} PO_4 and 47 μmol L^{-1} $Si(OH)_4$] to induce probable Fe-starved conditions
123 for the phytoplankton community before use. Nutrient stock solutions were passed through
124 Chelex-100 ion-exchange resin (Bio-rad) to remove trace metals (Morel et al., 1979). The
125 natural phytoplankton stock was incubated for 6 days in an on-deck incubator. The
126 temperature of the incubator was maintained at near-ambient sea surface temperature (~10°C)
127 by a surface seawater flow-through system. The incubator was covered with a single layer of
128 neutral density screening to achieve approximately 30% of surface irradiance.
129 The SPM_{DSW} was collected at 320 m depth east of Sakhalin (Stn DSW: 52°15′N,
130 144°35′E; Fig. 1) using an *in situ* filtration system (McLane Research Laboratories Inc.). The
131 DSW mass was detected by the anomalous values in low temperature (< ~0°C) with low
132 transmittance around the sigma-t = 26.8 kg m^{-3} layer as reported previously (Fukamachi et al.,
133 2004; Shcherbina et al., 2004). Approximately 454.5 L of DSW was filtered through a 1.0 μm
134 acid-washed polycarbonate filter (Nuclepore). The water on the filter was flushed by vacuum,
135 and the filter was frozen at −20°C for ~3 hours. Prior to the experiment, the SPM_{DSW} on the
136 filter was suspended in 500 mL of 0.2 μm filtered seawater (FSW) which was collected from
137 a depth of 200 m in the Oyashio region during the HK07-1 cruise aboard the R/V
138 Hokko-Maru (January 2007). The FSW contained 40 μmol L^{-1} NO_3+NO_2, 3.0 μmol L^{-1} PO_4,
139 63 μmol L^{-1} $Si(OH)_4$ and 0.88 nmol L^{-1} D-Fe. Six treatments were prepared as follows (Table
140 1): (1) control: 270 mL of FSW plus 45 mL of Fe-starved natural phytoplankton stock culture
141 prepared above; (2) Fe-added: added inorganic Fe to the control condition to make a final
142 concentration of 5 nmol L^{-1}; (3) DFB (desferrioxamine B): amended with 1 μmol L^{-1} DFB
143 (Sigma Chem. Co. Ltd.) to the control condition to prevent Fe uptake from the ambient
144 seawater as achieved previously (Wells, 1999; Iwade et al., 2006; Sugie et al. 2010b, 2011);
145 (4) SPM_{DSW}: 250 mL of FSW plus 45 mL of Fe-starved phytoplankton stock plus 20 mL of
146 resuspended SPM_{DSW} solution as prepared above, i.e., SPM_{DSW} was concentrated 63.5-fold vs.
147 *in situ* condition; (5) SPM_{DSW}−Phy: 295 mL of FSW plus 20 mL of resuspended SPM_{DSW}
148 solution without the addition of the Fe-starved phytoplankton stock; and (6) DSW_{raw}: 315 mL
149 of prescreened DSW using 100 μm acid-washed Teflon-mesh collected from 247 m at Stn
150 DSW (Table 1). The SPM_{DSW}−Phy treatment was intended to examine the viability of the

phytoplankton in the SPM_{DSW}, which was once frozen. The DSW_{raw} was set to elucidate the viability of phytoplankton in the DSW mass, which mimics their appearance to the sunlit surface waters by tidally induced and strong vertical mixing, such as that observed during winter (Nakamura and Awaji, 2004).

The treatments were incubated in an on-deck incubator as described above. The treatments were prepared in 9-replicate 320 mL polycarbonate bottles in addition to the DSW_{raw} treatment, which was prepared in 4-replicate. Three bottles were sacrificed and measured after 1, 3 and 5 days for analysis of macronutrients and Chl-*a* concentrations except for the samples of the DSW_{raw} treatment, which were obtained after 3 and 5 days sacrificing two bottles for each day. The concentrations of total dissolvable Fe (unfiltered; T-Fe) and background Fe in the FSW were measured at the beginning of the experiment. The samples for diatom cell densities and species compositions were collected at 0 and 5 days of incubation. Although the abundance of the small flagellates can be expected to be high in the incubation bottles, the large number of particles in the SPM_{DSW} and SPM_{DSW}−Phy treatments obscured the counts of the flagellates. Therefore, we measured only the diatom abundance using a light microscope. The experimental advantage of counting only diatoms to examine the availability of Fe in the SPM_{DSW} is that the diatoms are photolithoautotrophs, but some mixotrophic flagellates are capable of phagotrophic acquisition of P-Fe (Tortell et al., 1996; Maranger et al., 1998). Therefore, we can examine the availability of Fe potentially dissociated from the SPM_{DSW}. The Chl-*a* specific growth rate was calculated from the linear regression between the time (day) and the natural log of the Chl-*a* concentrations. For the Chl-*a* specific growth rate calculations, the data from the beginning to the end of the incubations were used for the control, DFB, SPM_{DSW}−Phy and DSW_{raw} treatments and those from day 1 to the end of the incubations were used for the Fe-added and SPM_{DSW} treatments. The growth rate in terms of cell numbers was calculated as follows: growth rate = $Ln(N_{d5} / N_{d0}) / 5$, where N_{d5} and N_{d0} represent cell numbers at day 5 and the start of the experiment, respectively.

2.2. Surface phytoplankton incubations

Seawater for incubation was collected at three sampling sites located at Stn Oy, in the Bussol' Strait (Stn BS: 46°30'N 151°23.2'E) and in the Sea of Okhotsk (Stn Ok: 47°30'N 150°20.45'E) (Fig. 1). Seawater samples were collected from 10 m depth using acid-cleaned Teflon-coated 10 L Niskin X sampling bottles. Seawater for experiments was sieved with 200 μm acid-cleaned Teflon-mesh to eliminate large mesozooplankton such as *Neocalanus* spp., which dominate in the western subarctic Pacific region (Ikeda et al., 2008). The prescreened seawater sample was homogenized in an acid-washed 20 L polycarbonate tank and then dispensed into acid-cleaned 320 mL polycarbonate bottles. The three treatments were conducted as follows: (1) unamended control; (2) Fe-added media with the addition of 5 nmol L^{-1} Fe; and (3) Fe-limited media with the addition of 1 μmol L^{-1} DFB. Fifteen bottles for each treatment were prepared and incubated in an on-deck incubator as described above. Three bottles were sacrificed at 1, 3, 5, 7 and 10 day intervals to measure the Chl-*a* concentration, phytoplankton abundance and macronutrient concentrations. The samples for the beginning of the experiment were taken from the residue in the 20 L tank. The Chl-*a* specific growth rate was calculated as described above using the Chl-*a* data from the beginning of the experiment for the control and the Fe-limited media, and from day 1 for the Fe-added media to the day before the nutrient depletions. The growth rate in terms of cell numbers was calculated using the same method as described in the SPM_{DSW} addition experiment.

2.3. Sample analysis

For measuring the Chl-*a* concentrations, the samples were filtered onto GF/F filters and measured with a Turner Design 10-AU fluorometer (Welschmeyer, 1994) after extraction with *N, N*-dimethylformamide (Suzuki and Ishimaru, 1990). The samples for macronutrient analysis during incubation were measured with a QuAAtro continuous flow analyzer (Bran+Luebbe). For Fe analysis, seawater samples were acidified at pH 3.2 with 10 mol L^{-1} formic acid and 2.4 mol L^{-1} ammonium formate buffer after the sample collection. The Fe concentration was measured with an automated Fe analyzer (Kimoto Electric) using a combination of an 8-hydroxyquinoline chelating resin concentration and luminol-hydrogen peroxide chemiluminescence detection with a closed flow-through system (Obata et al., 1993).

Unfiltered acidified samples were used to measure the total dissolvable Fe (T-Fe) and the samples passed through a 0.22 μm cartridge filter (Millipore) prior to formic acid and buffer addition were used to measure the dissolved Fe (D-Fe) (detection limit: < 0.05 nmol L^{-1} in this study). In the surface phytoplankton incubations, the Fe amount in the particulate fraction (P-Fe) was defined as follows: P-Fe = T-Fe − D-Fe. Note that the Fe in particulate form collected using an *in situ* filtration system (> 1.0 μm in diameter) during the SPM_{DSW} addition experiment is represented as $P\text{-}Fe_{DSW}$. The Fe concentrations were analyzed on-board immediately after the collection of the seawater samples at the beginning of the experiment. Our Fe measurement method was carefully assessed using SAFe (Sampling and Analysis of Fe) cruise reference standard seawater for an inter-comparison study distributed by the Moss Landing Marine Laboratory and University of California Santa Cruz. We measured 0.10 ± 0.010 nmol L^{-1} (n = 3) and 0.99 ± 0.023 nmol L^{-1} (n = 3) D-Fe by our method, respectively for concentrations of 0.094 ± 0.008 nmol L^{-1} (S) and 0.923 ± 0.029 nmol L^{-1} (D2) D-Fe (www.geotraces.org) for the reference standard seawater. For the phytoplankton cell count, seawater samples were fixed by formalin (1% final volume). An adequate volume of fixed seawater was poured into a settling chamber and allowed to settle for at least 24 hours (Hasle, 1978) for the day 0 sample, and centrifuged approximately 400×g for day 5 samples (Throndsen, 1978) before identification using a phase-contrast inverted microscope and light microscope, respectively. Diatom species were identified according to Hasle and Syvertsen (1997).

3. Results

3.1. SPM_{DSW} addition experiment

3.1.1. Hydrography

At Stn DSW, cold (< 0°C) and less saline (~33.3) intermediate water was detected around sigma-*t* = 26.8 kg m^{-3} (Fig. 2a, b, c), which was considered as OSIW (Fukamachi et al., 2004). Anomalously low beam transmission, i.e. high abundance of suspended particulate matter was detected below 245 m at Stn DSW (Fig. 2d).

3.1.2. Phytoplankton growth

Chl-*a* concentrations increased exponentially in the controls, Fe, and SPM_{DSW} treatments over the 5-day incubation period, whereas the concentrations decreased with time in the SPM_{DSW}−Phy treatment (Fig. 3a). The order of the maximum Chl-*a* concentrations during the incubation were as follows: SPM_{DSW} (60.9 ± 4.5 μg L^{-1}) > Fe-added (28.3 ± 3.8 μg L^{-1}) > control (18.9 ± 1.0 μg L^{-1}) > DFB (5.2 ± 0.2 μg L^{-1}) > DSW_{raw} (0.99 ± 0.2 μg L^{-1}) > SPM_{DSW}−Phy (0.14 ± 0.0 μg L^{-1}) (mean ± 1 SD of triplicate bottles or mean ± range of duplicate bottles). The Chl-*a* data in the SPM_{DSW}−Phy treatment indicated that most of the phytoplankton on the filter collected from the DSW died during the 3 hour freezing period. We then offset the Chl-*a* data for the SPM_{DSW} treatment by subtracting the value measured at each data point in the SPM_{DSW}−Phy treatment to calculate the specific growth rate. The specific growth rate was highest in the SPM_{DSW} (0.80 ± 0.03) (mean ± 95% C.L. of regression), followed by 0.66 ± 0.03 in the Fe-added, 0.59 ± 0.13 in the DSW_{raw}, 0.58 ± 0.02 in the control, 0.30 ± 0.02 in the DFB and −0.28 ± 0.09 in the SPM_{DSW}−Phy treatment (Fig. 3b). It is notable that the growth rate was the fastest (1.0 ± 0.09) during days 3 to 5 in the DSW_{raw} treatment as compared with all treatments.

At the beginning of the experiment, pennate diatom species such as *Pseudo-nitzschia* spp. and *Cylindrotheca closterium* / *Lennoxia faveolata* complex predominated relative to the centric diatoms (we detected mainly *Chaetoceros* spp. subgenus *Phaeoceros*) in the possibly Fe-starved Oyashio phytoplankton community (Table 2). In the treatments without the addition of Oyashio phytoplankton (SPM_{DSW}−Phy and DSW_{raw}), the centric (mainly *Chaetoceros* spp. subgenus *Hyalochaete* and *Thalassiosira* spp.) and pennate diatoms (mainly *Thalassionema nitzschioides*) dominated, and they contributed equally (Table 2). In addition, *Hyalochaete* spp. resting spores were detected in the DSW_{raw} treatment at levels of 80 spores L^{-1}. It should be noted that the species in the SPM_{DSW} and DSW_{raw} treatments were considered as mainly coastal diatoms (Hasle and Syvertsen, 1997). At day 5, abundances of the pennate diatoms were three orders of magnitude higher than those of the centric species in the Oyashio phytoplankton-added treatments, except for the DFB treatment, whereas in the DSW_{raw} treatment, *Hyalochaete* spp., *Thalassiosira* spp., *T. nitzschioides*, and, notably, resting spore-forming species such as *Thalassiosira antarctica* ver. *borealis* and *Ditylum brightwellii* were observed. The total diatom abundance at the end of the incubations was the

following order: SPM_{DSW} > Fe-added > control > DFB >> SPM_{DSW}−Phy ≈ DSW_{raw} (Table 2). This order is nearly identical to that of the maximum Chl-*a* concentrations (Fig. 3a). The net growth rates during the 5 day incubation period were similar between centric and pennate diatoms in the control, SPM_{DSW} and DSW_{raw} treatments, whereas that of the pennate diatoms was faster than that of the centric diatoms in the Fe-added treatment (Table 4). In the DFB-added treatment, the net growth rate of diatoms and flagellates was slower than that in the controls and Fe-added treatments.

3.1.3. Nutrient dynamics

The T-Fe concentrations in the control (≈ DFB) and SPM_{DSW} (≈ SPM_{DSW}−Phy) treatments were 0.93 and 47.7 nmol L^{-1}, respectively. The concentration of P-Fe_{DSW} (> 1.0 μm) is derived as an approximation based on the measurement of the concentrated SPM in the experimental bottles. Thus, the P-Fe_{DSW} concentration was 0.83 nmol L^{-1} in the *in situ* DSW (320 m) mass at Stn DSW. Macronutrient concentrations at the beginning of the experiment were 30.0–48.6 μmol L^{-1} DIN (NO_3+NO_2+NH_4^+), 2.48–3.86 μmol L^{-1} PO_4, and 56.7–74.1 μmol L^{-1} $Si(OH)_4$. None of the nutrients were exhausted over the course of the experiment; for example, DIN remained at 31.7, 24.4, 40.0, 12.3, 42.1 and 28.8 μmol L^{-1} in the control, Fe, DFB, SPM_{DSW}, SPM_{DSW}−Phy and DSW_{raw} treatments, respectively. During the 5 day incubation, nutrients seemingly increased with time in the SPM_{DSW}−Phy treatment probably due to the dissolution from the added SPM_{DSW} without a substantial biological uptake. Nutrient drawdown in the SPM_{DSW} treatment was offset by subtracting the value measured in the SPM_{DSW}−Phy treatment (Table 3). The order of the amount of nutrient drawdown was the same as that of the increase in Chl-*a* concentrations (Fig. 3). The Si:N drawdown ratio was higher in the SPM_{DSW} compared to that of the control and Fe-added conditions (Table 3). The Si:P drawdown ratio in the SPM_{DSW} treatment was nearly the same as that of the canonical value for vegetative growing diatoms (Brzezinski, 1985), whereas the values in the control and Fe-added treatments were smaller than that in the SPM_{DSW} treatment. In the DFB treatment, no Si drawdown and low N:P drawdown ratio were measured. The nutrient drawdown in the DSW_{raw} treatment was too small to calculate the drawdown ratios correctly (Table 3).

300

301 3.2. Surface phytoplankton incubations

302 3.2.1. Hydrography

303 At the beginning of the three experiments, the upper mixed layer depth was
304 approximately 30, 30 and 20 m at Stns Oy, BS and Ok, respectively (Fig. 4), which was
305 estimated from the first downward increase in sigma-$t \geq 0.02$ m^{-1}. The stratifications were
306 weaker at Stns BS and Ok as compared to Stn Oy. At the Stn Oy site, the hydrographic
307 conditions were typical of the Western Subarctic Gyre (WSG) during summer, with less
308 saline waters (~32.6) in the surface, with dichothermal water at around 100 m depth or 26.6
309 kg m^{-3} sigma-*t* (e.g., Yasuda et al., 2002) (Fig. 4). Hydrographic conditions at Stns BS and
310 Ok were intermediate between those of the WSG (Stn Oy) and the Okhotsk waters (Stn DSW;
311 Fig. 2). The sigma-*t* values at Stns BS and Ok were vertically homogenous from ~150 down
312 to 500 m and from ~50 down to 700 m, respectively (data not shown), probably due to the
313 effect of intensive vertical water mixing around the Bussol' Strait. The NO_3+NO_2
314 concentrations at 10 m depth used in the incubation experiment were 8.8, 18.9 and 13.8 µmol
315 L^{-1} at Stns Oy, BS and Ok, respectively. The D-Fe concentrations at 10 m were < 0.05, < 0.05
316 and 0.10 nmol L^{-1}, and the T-Fe concentrations were < 0.05, 0.51 and 0.18 nmol L^{-1} at Stns
317 Oy, BS and Ok, respectively.

318

319 3.2.2. Phytoplankton growth

320 At all stations, Fe addition stimulated phytoplankton growth compared to the unamended
321 controls (Fig. 5a, b, c). At the beginning of the experiment, the total diatom abundance was
322 the highest at Stn BS (19,500 cells L^{-1}) followed by Stns Ok (12,400 cells L^{-1}) and Oy (8,400
323 cells L^{-1}) (Fig. 6). The small pennate diatom *C. closterium* / *L. faveolata* complex (apical
324 axis: 10–20 µm, transapical axis: <1 µm, equivalent spherical diameter (ESD): ~2–4 µm),
325 was predominant in the bottles at all stations. Other dominant species were also small:
326 *Fragilariopsis* spp. (ESD: 2.5–6 µm) and a narrow group of *Pseudo-nitzschia* spp. (ESD: ~4
327 µm) (Fig. 6). The abundances of microscopically identifiable small flagellates (ESD: ~3–10
328 µm) were 3 (Stn BS) to 25 (Stn Ok) times higher than those of the diatoms. During the
329 incubation experiment, small pennate diatoms, especially *C. closterium* / *L. faveolata*

complex and *Pseudo-nitzschia* spp., prominently increased in all treatments (Table 4). Interestingly, at Stns Oy and BS, the growth rate of the centric diatoms was not enhanced by the addition of Fe, whereas that of the pennate diatoms and flagellates were faster in the Fe-added treatment at all stations (Table 4). The enhancement effect on the growth rates through the addition of Fe, calculated from cell abundance, was smaller than that due to Chl-*a* (Table 4). In the DFB-added treatment, the Chl-*a* concentration was unchanged at Stn Oy and increased slightly at Stns BS and Ok. Diatom and flagellate abundance increased after the addition of DFB, although the growth rates were smaller than in the controls (Table 4).

3.2.3. Nutrient dynamics

The NO_3+NO_2 drawdown reflected the Chl-*a* increases; the most rapid drawdown was obtained with the Fe-added treatments, followed by the controls and the DFB treatments (Fig. 5d, e, f). The trends in PO_4 utilization were the same as those of NO_3+NO_2 (data not shown). Ammonium utilization varied among the three stations but was statistically insignificant among the experimental treatments; it gradually decreased from 0.54 to ~0.2 μmol L^{-1} and 0.78 to ~0.2 μmol L^{-1} at Stn Oy and Ok, respectively, and remained constant at ~0.2 μmol L^{-1} at Stn BS. The variations in $Si(OH)_4$ concentrations were almost identical in the controls and Fe added treatments and less utilized in the DFB treatments compared to the other treatments (Fig. 5g, h, i). The Si:N drawdown ratio decreased by the addition of Fe compared to what was observed in the controls at Stns Oy, BS and Ok: 0.12 ± 0.05, 0.42 ± 0.05 and 0.28 ± 0.01 (mean ± 1 SD of triplicate bottles) in Fe-added treatments and 0.45 ± 0.00, 0.78 ± 0.09 and 0.37 ± 0.10 in the controls, respectively. In the DFB treatments, the Si:N ratio was the highest among three treatments ranging from 1.05 (Stn Ok) to 1.53 (Stn Oy).

3.2.4. Effect of Fe manipulation

Four indexes were calculated to examine the Fe nutritional status of phytoplankton (Fig. 7). First, the relative specific growth rate, calculated from the Chl-*a* data for the controls ($\mu_{control}$) and divided by that for the Fe-added treatment ($\mu_{Fe\text{-}added}$), was used as an indicator of apparent bioavailability of all available Fe sources in the control bottles. The $\mu_{control}/\mu_{Fe\text{-}added}$

ratio was significantly smaller at Stn Oy (0.42 ± 0.07) compared to Stn BS (0.66 ± 0.06), whereas the values were not statistically significant between Stns Oy and Ok (0.64 ± 0.12) and Stns BS and Ok (Dunnet *t*-test, $p > 0.05$; Fig. 7a). Second, we calculated ΔChl-*a* by subtracting the increase in Chl-*a* in the DFB treatment from that of the controls as an index of Fe utilized from the extracellular fraction. It should be noted that phytoplankton such as diatoms acclimated in an Fe-depleted medium with amended DFB-Fe as a sole Fe source can utilize Fe from a DFB-Fe complex via cell surface metalloreductases (Maldonado and Price, 2001; Shaked et al., 2005; Strzepek et al., 2011). This suggests that the utilized extracellular Fe is underestimated due to an overestimation of the Fe in the intracellular fraction. However, the Fe uptake from the DFB-Fe complex is very small, and the Fe taken up by the cells is too small to support Chl-*a* synthesis under an extremely high DFB:Fe ratio in seawater (Wells, 1999; Yoshida et al., 2006; Sugie et al., 2011). The ΔChl-*a* was smallest at Stn Oy (6.0 ± 0.1 μg L^{-1}) followed by Stn Ok (6.5 ± 1.1 μg L^{-1}) and Stn BS (10.2 ± 0.8 μg L^{-1}) during a 10 day incubation period (Fig. 7b). The third and fourth indices are ΔNO_3+NO_2 and ΔNH_4^+, which were calculated by subtracting the NO_3+NO_2 and NH_4^+ drawdown in the DFB treatment from that of the controls (Fig. 7c and 7d). These indices are similar proxies to that of ΔChl-*a* as stated above. The trend in ΔNO_3+NO_2 was similar to the relative growth rate of $\mu_{control}/\mu_{Fe\text{-}added}$ (Fig. 7a) and ΔChl-*a* (Fig. 7b); it was higher at Stn BS (12.7 ± 1.2 μg L^{-1}) as compared to Stns Ok (9.3 ± 1.2 μmol L^{-1}) and Oy (8.1 ± 0.4 μmol L^{-1}; Fig. 7c). The ΔNH_4^+ was less than 0.1 μmol L^{-1} at all stations (Fig. 7d).

4. Discussion

4.1. Bioavailability of Fe in the SPM_{DSW}

The present study is the first clear demonstration that particulate matter (> 1 μm) collected in the nepheloid layer can supply bioavailable Fe that can promote the growth of phytoplankton such as diatoms. The base FSW, which was collected from a depth of 200 m in the Oyashio region, should contain ample nutrients and other trace elements except for Fe, and measurable nutrients remained in all treatments at the end of the experiment. Furthermore, NH_4^+, which potentially promotes the growth of phytoplankton, was constant at ~0.3 μmol L^{-1} in the SPM_{DSW}−Phy treatment throughout the experiment. This suggests that

390 remineralized elements other than Fe, such as other trace metals and nutrients, did not affect
391 the growth of phytoplankton in the SPM_{DSW}-added treatments (c.f., Coale, 1991). The higher
392 Chl-*a* concentration and diatom abundance, with slightly faster growth rates in the SPM_{DSW}
393 treatment than the Fe-added treatment, may signify that Fe from the SPM_{DSW} was supplied
394 immediately at a higher concentration than 5 nmol L^{-1} or a higher bioavailability of Fe,
395 compared to added inorganic Fe, a large part of which is considered as solid phase inorganic
396 Fe. However, it is very difficult to compare the bioavailability of Fe in the SPM_{DSW} with that
397 in solid inorganic Fe oxyhydroxide because of the extremely different Fe concentration in the
398 media used in the present study. The rapid growth of phytoplankton in the DSW_{raw} treatment
399 during the 3 to 5 day incubation period partially supports the possibility that P-Fe_{DSW} in the
400 DSW mass was highly bioavailable. It should be noted that it is likely that the high
401 concentration of SPM_{DSW} interferes with the grazing pressure of microzooplankton (Price et
402 al., 1994), which could have enhanced the net growth rate further in the SPM_{DSW} treatment as
403 compared to the Fe-added treatment. In addition, we observed resting spores of *Hyalochaete*
404 spp. at the beginning of the DSW_{raw} treatment, which showed the fastest growth rate among
405 the treatments with a few days of lag period (Fig. 3a). Diatom resting spores are an ecological
406 strategy in order to survive under unfavorable conditions for growth (e.g., Sugie et al., 2010b),
407 and they can germinate rapidly after appearing under favorable conditions (McQuoid and
408 Hobson, 1996). We suggest that the resting spore-forming coastal diatoms contributed to the
409 fast growth of the centric species in the DSW_{raw} treatment with bioavailable Fe sources.
410 It has been well documented that the bioavailability of inorganic P-Fe for
411 photolithoautotrophs depends on the surface reactivity of the solid inorganic Fe oxyhydroxide
412 species (Kuma and Matsunaga, 1995; Chen and Wang, 2000; Yoshida et al., 2006). The
413 reactivity of solid inorganic Fe oxyhydroxide decreases with an increase in aging time and
414 temperature and depends on the crystal structure (Kuma and Matsunaga, 1995; Yoshida et al.,
415 2006). The temperature in the DSW is low (< 0°C: e.g. Fukamachi et al., 2004), and hence,
416 the bioavailability of Fe in the SPM_{DSW} may be kept high for a long time if the P-Fe_{DSW} is
417 composed of inorganic substances. Alternatively, the DSW is rich in organic detritus possibly
418 derived from intensive diatom production on the continental shelf of Sakhalin Island
419 (Nakatsuka et al., 2004). Such detritus can release Fe-binding ligands such as humic

substances during particulate remineralization in the water column by bacteria and photodissolution by irradiance in the surface layer (Mayer et al., 2009; Boyd et al., 2010). It has been reported that Fe complexes with humic type ligands are highly bioavailable, similar to inorganic Fe(III) for marine phytoplankton (Chen and Wang, 2008). In other cases, if bioactive Fe can be incorporated into or onto colloidal matrices, and then become enhanced in the particulate phase by the progressive sorption of other organic colloids with cation bridges (Wells, 2002), the Fe in the particles may become bioavailable after bacterial remineralization and/or photodissolution (Boyd et al., 2010). The effect of the short-term freezing of the SPM_{DSW} caused cell death of the phytoplankton, which may also enhance remineralization of the Fe from the SPM_{DSW} because Fe released from the dead phytoplankton potentially is of high bioavailability (Poorvin et al., 2004). In addition, a recent study reported that marine polysaccharides are important Fe-binding ligands in the colloidal fraction and that the Fe bound to polysaccharides is of high bioavailability for phytoplankton (Hasser et al., 2011). Polysaccharides are known as a precursor of transparent exopolymer particles, which are believed to be bridges to create large aggregates (Passow, 2002). These above possibilities allow us to assume that the highly bioavailable Fe could be retained in the particulate phase for a suitable length of time associated with organic matters in the DSW and OSIW. However, the bioavailability of Fe in the SPM_{DSW} may decrease with aging time during transport and with the increase in temperature when it is drawn into the surface mixed layer. Further experiments are needed to determine the accurate chemical state and bioavailability of P-Fe collected from various regions in the western subarctic Pacific with more realistic concentrations added to phytoplankton communities.

4.2. Phytoplankton dynamics and their available Fe sources in the surface waters

The addition of Fe enhanced phytoplankton growth in terms of Chl-*a* at all three stations indicating phytoplankton nutritional status was clearly Fe-limited in the control bottles. However, phytoplankton growth measured with cell abundances was consistently faster than that measured with Chl-*a* concentrations (Figs. 3, 5 and Tables 2, 4). The difference between the growth rate calculated from the Chl-*a* and diatom cell density was caused by the gradual decrease in the intracellular Chl-*a* concentration of the phytoplankton

450 over the incubation period (Sugie et al., 2011). The Chl-*a* cell quota was also affected due to
451 light conditions, which may differ between *in situ* and incubation conditions. It should also be
452 noted that bulk Chl-*a* concentration values reflect the whole community, while cell counts
453 target specific populations. This may also contribute to differences in growth rate determined
454 via Chl-*a* vs. cell counts.

455 The Si:N drawdown ratios of the Fe added bottles decreased compared to that of the
456 controls suggesting some contribution from diatoms, especially at Stn Oy, and their recovery
457 from iron-limited conditions, which leads to a high Si:N drawdown ratio (Takeda, 1998;
458 Sugie et al., 2010b). The growth rate of pennate diatoms was enhanced during all experiments,
459 whereas the growth of centric species was promoted in only one (Stn Ok) out of four
460 experiments (Tables 2, 4). The growth rates of centric diatoms, where the stations had a
461 dominance of oceanic *Phaeoceros* spp., were not enhanced by the addition of Fe. In contrast,
462 the phytoplankton community at Stn Ok had a relatively high abundance of coastal centric
463 diatoms such as *Hyalochaete* spp. and *Thalassiosira* spp. compared to the other stations (Fig.
464 6), which may have contributed to an increase in the growth rate of the centric diatom in
465 response to the addition of Fe. Strezepek and Harrison (2004) reported that oceanic species
466 cannot adapt quickly to rapid changes in external environments due to the trade-off between
467 adaptability vs. the capacity to survive under relatively permanent, Fe-limited oceanic
468 conditions. In addition, surge Fe uptake upon Fe addition and subsequent storage using
469 ferritin are considered to be an advantageous strategy of pennate diatom (Marchetti et al.,
470 2009). Our results support previous suggestions that pennate diatoms are better able to
471 increase growth rate with the addition of inorganic Fe in relative to oceanic centric diatoms
472 (Table 4). Ecophysiological strategies in the Fe utilization of phytoplankton appear to be one
473 of the most important factors controlling phytoplankton dynamics in oceanic Fe-limited
474 regions.

475 At the beginning of the surface water incubations (i.e., reflecting *in situ* condition),
476 the Chl-*a* concentrations were relatively high (0.85 to 1.58 μg L^{-1}) compared to oceanic
477 HNLC regions such as the central subarctic gyres and the equatorial Pacific region (e.g., Price
478 et al., 1994; Nishioka et al., 2003). The net growth rate in the unamended controls calculated
479 from the Chl-*a* data and diatom cell density ranged from 0.20 to 0.31 d^{-1} (Fig. 5) and 0.69 to

480 1.34 d^{-1} (Table 4), respectively. These results indicate that the *in situ* phytoplankton
481 communities were mildly Fe-limited, which may explain the moderately high Chl-*a*
482 concentrations in the surface waters even under D-Fe depleted conditions. Yoshimura et al.
483 (2010) also reported that the phytoplankton community in the Bussol' Strait in 2006, at
484 virtually the same location as Stn BS in this study, was under a Fe-limited or Fe- and
485 light-co-limited condition. Although D-Fe concentrations were near depletion at the
486 beginning of the incubations, phytoplankton biomass increased in the controls, with the
487 $\mu_{control}/\mu_{Fe\text{-}added}$ ranging from 0.42 to 0.66. In the DFB treatments, which eliminated almost all
488 external Fe from the bioavailable fraction to phytoplankton, the net Chl-*a* increase and
489 NO_3+NO_2 drawdown were less than those in the controls (Fig. 7). It suggests that further
490 growth of phytoplankton in the control bottles was not only supported by Fe in the
491 intracellular fraction but also by the extracellular fractions.
492 The possible bioavailable Fe source for the phytoplankton was the particulate phase
493 under the D-Fe depleted conditions. We estimated the utilization of intra- and extracellular Fe,
494 which can be distinguished by calculating the increase of Chl-*a* and the NO_3+NO_2 and NH_4^+
495 drawdowns in the controls minus that of the DFB-added treatment (hereafter referred to as
496 ΔChl-*a*, ΔNO_3+NO_2 and ΔNH_4^+, respectively; Fig. 7b, c, d). However, we cannot estimate the
497 extracellular fraction of utilized Fe at Stn Oy due to the fact that both D-Fe and T-Fe
498 concentrations were below the detection limit. The utilized Fe in the extracellular source was
499 potentially underestimated because we did not take into account the Fe uptake from the
500 DFB-Fe complex (e.g., Maldonado and Price, 1999, 2001; Strezepek et al., 2011). However
501 as stated earlier, the Fe uptake and subsequent cell or Chl-*a* growth should be very small for
502 an extremely high DFB:Fe ratio (1 μmol L^{-1}:< 0.05–0.5 nmol L^{-1} (T-Fe)), as observed in
503 previous studies (Wells, 1999; Iwade et al., 2006; Sugie et al., 2011).
504 First, we calculated the potential Fe requirement of the phytoplankton in the control
505 bottles from the extracellular fraction using the ΔChl-*a* values during the incubations and
506 reported Fe:Chl-*a* values. The Fe:Chl-*a* ratio was calculated from the Fe:C ratio (μmol:mol)
507 divided by the Chl-*a*:C ratio (g:mol) applied from reported values (Table 5). The Fe:Chl-*a*
508 value of the Fe-limited oceanic phytoplankton ranged from 4.7 to 108 μmol g^{-1} (Table 5). In
509 this study, phytoplankton communities at Stns BS and Ok were Fe-limited; consequently, we

510 selected these ratios determined only under Fe-limited conditions. Because the contribution
511 of coastal species was small (~2% at Stn BS and ~8% at Stn Ok), we used the reported values
512 obtained from oceanic phytoplankton species. Although these values were measured through
513 unialgal culture experiments using nano- and micro-sized phytoplankton, we had no
514 information regarding accurate Fe:Chl-*a* values in the natural phytoplankton community and
515 pico-sized phytoplankton. The reported Fe:C values of the oceanic phytoplankton used in the
516 above calculation was similar to that of natural oceanic phytoplankton in Fe-limited HNLC
517 regions (Table 5). It should be noted that the estimated Fe requirement may be potentially
518 overestimated because the Fe requirements of pico-phytoplankton, which may contribute
519 substantial biomass in the bottles, is believed to be small relative to that of larger
520 phytoplankton (Timmermans et al., 2005). However, the size dependence of the Fe:C ratio is
521 still in debate; Strzepek et al. (2011) reported that the Fe:C ratio increased with a decrease in
522 cell volume. According to the stoichiometric calculation, the phytoplankton community at Stn
523 BS under the D-Fe depleted (< 0.05 nmol L^{-1}) and P-Fe (0.5 nmol L^{-1}) conditions required
524 0.05 to 1.10 nmol L^{-1} Fe from extracellular sources. The D-Fe (0.10 nmol L^{-1}) at Stn Ok
525 could support the growth of a phytoplankton community in the control bottles (required 0.03
526 to 0.71 nmol L^{-1}) only when applied to the lowest Fe:Chl-*a* value. The presence of the coastal
527 diatom species would tend to increase Fe demand from the extracellular fraction due to their
528 high Fe requirements compared to the oceanic species (Table 5).
529 Second, we calculated another index for the community Fe requirement from the
530 extracellular fraction in the controls using the data on ΔNO_3+NO_2 and ΔNH_4^+ values. The
531 nitrogen utilizations were converted into carbon biomass using the canonical Redfield ratio
532 (Redfield et al., 1963). The variation in C:N ratio caused by changing the availability of Fe is
533 rather small compared to Fe:C ratios (e.g., Price, 2005; Sugie and Yoshimura, in press). The
534 decrease in Fe requirements of phytoplankton using NH_4^+ relative to NO_3 utilization was
535 taken into account according to the theoretical calculations of Raven (1988). The Fe:C ratios
536 of the Fe-limited phytoplankton applied ranged from 0.4 to ~10 μmol mol^{-1} (Table 5). The
537 Fe:C ratios fall in the minimum to intermediate values of phytoplankton Fe requirements
538 determined for unialgal culture and *in situ* phytoplankton and seston (Table 5). The
539 phytoplankton community required 0.03–0.84 and 0.02–0.62 nmol L^{-1} Fe at Stns BS and Ok,

540 respectively, with <0.05 and 0.10 nmol L^{-1} D-Fe and ~0.50 and 0.08 nmol L^{-1} P-Fe
541 concentrations *in situ*, respectively.

542 These above estimations suggest that observed phytoplankton growth in control
543 experiments at both Stns BS and Ok could not have been supported by only the D-Fe phase.
544 Fitzwater et al. (2003) reported that ~10% of Fe in the particulate phase was labile (leachable
545 by 25% acetic acid for 2h) and that labile particulate Fe may contribute to the growth of
546 phytoplankton through Fe remineralization. In addition, a recent model study suggested that
547 the phytoplankton community in the Oyashio region of the western subarctic Pacific
548 compensates their Fe demand from remineralization and/or desorption processes via the
549 particulate phase during the summer (Shigemitsu et al., 2012). Our empirical calculations
550 support the previous measurements (Fitzwater et al., 2003) and estimations (Elrod et al.,
551 2008; Nakayama et al., 2010; Sugie et al., 2010a) that a significant portion of the Fe in the
552 particulate phase is bioavailable. Although some latent uncertainties in the stoichiometric
553 calculation remain, the Fe in the particulate phase is an important Fe source for a
554 phytoplankton community under D-Fe depleted conditions. Previous studies reported that the
555 possible bioavailability of Fe in the particulate phase would change due to the variability of
556 the source of SPM (Fitzwater et al., 2003; Elrod et al., 2008). Note that the source of SPM
557 around the Bussol′ Strait most likely originates from coastal regions of the Sea of Okhotsk
558 (see below), not from the Kurile Islands due to the very narrow continental shelves with steep
559 trenches (Fig. 1). The bioavailability of Fe in the particulate fraction derived from different
560 sources and regions is an important issue to clarify in understanding the variability of Fe
561 bioavailability in coastal and oceanic waters. Furthermore, the remineralization rate for Fe in
562 the various sources of SPM is critically important to better understand the biogeochemical
563 cycle of Fe and other nutrients in the ocean.
564
565 4.3. Possible role of SPM_{DSW} around the Kuril Strait
566 The Fe in the SPM_{DSW} was apparently bioavailable for phytoplankton, as shown in
567 the present study. Previous field observations and model work indicated that a high Fe water
568 mass would be transported from the OSIW originating from coastal regions of the Sea of
569 Okhotsk to the western North Pacific region via the Bussol' Strait (Nishioka et al., 2007;

570 Misumi et al., 2011). In the present study, deep vertical mixing was observed at Stns BS and
571 Ok; mixing around the Kuril Straits is a common phenomenon (e.g., Ito et al., 2010, 2011;
572 Yoshimura et al., 2010). Therefore, a substantial portion of Fe, especially P-Fe in the surface
573 near Stns BS and Ok, may be considered to be derived from the OSIW, the residence time of
574 which is considered to be a few years (Yamamoto et al., 2001). The availability of P-Fe in
575 OSIW and DSW would be substantially prolonged, possibly due to the formation of
576 Fe-organic associations as suggested above, and the cold characteristic of the OSIW mass
577 (<1°C) may also support the bioavailability of Fe for a long time (Kuma et al., 2000). Recent
578 studies also indicated that the contribution of lithogenic Fe to the total Fe in the SPM (>1 μm)
579 collected from the OSIW with the same *in situ* filtration system as the present study decreased
580 from Sakhalin Island toward the Bussol′ Strait (Shigemitsu, unpublished data). This suggests
581 that a substantial part of the P-Fe around the Bussol′ Strait is associated with organic
582 materials, which may be available for phytoplankton as observed in the present study. These
583 above physical and chemical factors potentially enable phytoplankton to utilize bioavailable
584 P-Fe in the surface mixed layer even with the relatively long residence time of the OSIW. In
585 future work, we should examine to what extent the bioavailability of P-Fe is prolonged and
586 the importance of bioavailable P-Fe in the western subarctic Pacific regions where P-Fe
587 contributes to relatively rich environments (Nishioka et al., 2003; Kitayama et al., 2009;
588 Nakayama et al., 2010). In addition, it should be noted that phytoplankton in the DSW mass
589 showed healthy growth (μ = 1.0 d^{-1}), with a lag period of a few days as observed in the
590 DSW_{raw} treatment. The short lag time could stem from the presence of resting spore-forming
591 diatoms such as *Hyalochaete* spp., *T. antarctica* ver. *borealis* and *D. brightwellii*, which
592 require a few days for germination (c.f., McQuoid and Hobson, 1996). The seed population of
593 coastal diatoms is transported around the Kuril Islands with the southeasterly flow of the
594 OSIW. Yoshimura et al. (2010) reported that coastal diatom species such as *Thalassiosira* spp.
595 dominated among the diatoms at the end of the incubation experiment conducted near Stn BS
596 in August 2006, when the water column mixed down to ~800 to 1000 m without surface
597 stratification. We also observed an increase in the coastal diatom species, with high net
598 growth rates ranging from 0.78 to 1.1 d^{-1} when using seawater collected from 50, 200, 500
599 and 1000 m depths at Stns Oy, BS and Ok for incubation (Sugie, unpublished data). Such

coastal diatom species are clearly different from the summer phytoplankton community in the open western subarctic Pacific regions (Aizawa et al., 2005; Komuro et al., 2005). The complex physical conditions in the Sea of Okhotsk may be able to sufficiently host allochthonous coastal phytoplankton around the Kuril Straits, possibly originating from the pelagic realm of the inner part of the Sea of Okhotsk. Furthermore, nutrients, especially $Si(OH)_4$ dissolved from the SPM_{DSW} as revealed from the data in the SPM_{DSW}−Phy treatment, partly enhance nutrient concentrations in the intermediate water. Nevertheless, we still need to quantify the accurate remineralization rate for nutrients dissolved from the SPM_{DSW} with a longer experimental period and low temperatures. If the SPM_{DSW}-like particles were transported to the Kuril Straits region and subsequent diapycnal mixing occurred (Nakamura and Awaji, 2004), then bioavailable P-Fe (i.e., $P\text{-}Fe_{DSW}$ or SPM_{DSW}) and healthy coastal phytoplankton could partly emerge to the sunlit surface waters associated with macronutrients and bioavailable D-Fe. Such bio-active elements and allochthonous phytoplankton populations supplied by mixing events seemingly support high productivity and biodiversity around the Kuril Straits. In addition, the bioavailability of P-Fe for phytoplankton other than diatoms is an important issue because they play a major role in the D-Fe-depleted oceanic regions of the North Pacific Oceans during the summer (e.g., Suzuki et al., 2002).

Contributors

K.S., J.N., K.K., Y.N.V. and T.N. designed research; K.S., J.N. and T.N. performed research; K.S. and J.N. analyzed data; K.S. wrote the paper and J.N., K.K. and T.N. assisted drafting.

Acknowledgement

We would like to thank the captain and crews of the R/V Professor Khromov for their efforts at sea. We are grateful to the extensive support from the Amur-Okhotsk projects at the Research Institute for Humanity and Nature (RIHN), especially Dr. T. Shiraiwa, leader of this Project, and Dr. Y.N. Volkov, Director of Far Eastern Regional Hydrometeorological Research Institute, Vladivostok, Russia. We acknowledge two anonymous reviewers for providing valuable comments, which significantly improved the paper. We also thank Ms. E.

630 Manabe at the Hokkaido University for technical support. Dr. M. Shigemitsu in the Hokkaido
631 University kindly provided the unpublished data and a fruitful discussion, which significantly
632 supported our observations.
633
634 References
635 Aizawa, C., Tanimoto, M., Jordan, R.W., 2005. Living diatom assemblages from North
636 Pacific and Bering Sea surface water during summer 1999. Deep-Sea Res. II 52,
637 2186–2205. doi:10.1016/j.dsr2.2005.08.008.
638 Anderson, M.A., Morel, F.M.M., 1982. The influence of aqueous iron chemistry on the
639 uptake of iron by the coastal diatom *Thalassiosira weissflogii*. Limnol. Oceanogr. 27,
640 789–813.
641 Boyd, P. W., Ibisanmi, E., Sander, S. G., Hunter, K. A., Jackson, G. A., 2010.
642 Remineralization of upper ocean particles: Implications for iron biogeochemistry.
643 Limnol. Oceanogr. 55, 1271–1288. doi:10.4319/lo.2010.55.3.1271.
644 Brzezinski, M.A. 1985. The Si:C:N ratio of marine diatoms: interspecific variability and the
645 effect of some environmental variables. J. Phycol. 21, 347–357.
646 Chen, M., Wang, W.-X., 2008. Accelerated uptake by phytoplankton of iron bound to humic
647 acids. Aquat. Biol. 3, 155–166. doi:10/3354/ab00064.
648 Coale, K.H., 1991. Effects of iron, manganese, copper, and zinc enrichments on productivity
649 and biomass in the subarctic Pacific. Limnol. Oceanogr. 36, 1851–1864.
650 Elrod, V.A., Johnson, K.J., Fitzwater, S.E., Plant, J.N., 2008. A long-term, high-resolution
651 record of surface water iron concentrations in the upwelling-driven central California
652 region. J. Geophys. Res. 113, C11021, doi:10.1029/2007JC004610.
653 Fitzwater, S.E., Johnson, K.S., Elrod, V.A., Ryan, J.P., Coletti, L.J., Tanner, S.J., Gordon,
654 R.M., Chavez, F.P., 2003. Iron, nutrient and phytoplankton biomass relationships in
655 upwelled waters of the California coastal system. Cont. Shelf Res. 23, 1523–1544.
656 Fukamachi, Y., Mizuta, G., Ohshima, K.I., Talley, L.D., Riser, S.C., Wakatsuchi, M., 2004.
657 Transport and modification processes of dense shelf water revealed by long-term
658 moorings off Sakhalin in the Sea of Okhotsk, J. Geophys. Res. 109, C09S10,
659 doi:10.1029/2003JC001906.

660 Hasle, G.R., 1978. Using the inverted microscope. In: Sourina, A. (Ed.), Phytoplankton
661 manual. UNESCO, Paris, p. 191–196.
662 Hasle, G.R., Syvertsen, E.E., 1997. Marine diatoms. In: Tomas, C.R., (Ed.), Identifying
663 Marine Phytoplankton. Academic Press, London, p. 5–385.
664 Hassler, C.S., Schoemann, V., 2009. Bioavailability of organically bound Fe to model
665 phytoplankton of the Southern Ocean. Biogeosciences 6, 2281–2296.
666 Hassler, C.S., Schoemann, V., Nichols, C.M., Butler, C.V., Boyd, P.W., 2011. Saccharides
667 enhance iron bioavailability to Southern Ocean phytoplankton. Proc. Natl. Acad. Sci.
668 U.S.A. 108, 1076–1081. doi:10.1073/pnas.1010963108.
669 Hutchins, D.A., Franck, V.M., Brzezinski, M.A., 1999a. Inducing phytoplankton iron
670 limitation in iron-replete coastal waters with a strong chelating ligand. Limnol.
671 Oceanogr. 44, 1009–1018.
672 Hutchins, D.A., Witter, A.E., Bulter, A., Luther III, G.W., 1999b. Competition among marine
673 phytoplankton for different cheleted iron species. Nature 400, 858–861.
674 Ikeda, T., Shiga, N., Yamaguchi, A., 2008. Structure, biomass distribution and
675 trophodynamics of the pelagic ecosystem in the Oyashio region, western subarctic
676 Pacific. J. Oceanogr. 64, 339–354.
677 Ito, S., Yasuda, I., Nakatsuka, T., Nishioka, J., Volkov, Y.N., 2010. Fine- and microstructure
678 observations in the Urup Strait, Kuril Islands, during August 2006. J. Geophys. Res. 115,
679 C08004. doi:10.1029/2009JC005629.
680 Ito, S., Yasuda, I., Yagi, M., Osafune, S., Kaneko, H., Nishioka, J., Nakatsuka, T., Volkov,
681 Y.N., 2011. Strong vertical mixing in the Urup Strait. Geophys. Res. Lett. 38, L16607.
682 doi:10.1029/2011GL048507.
683 Iwade, S., Kuma, K., Isoda, Y., Yoshida, M., Kudo, I., Nishioka, J., Suzuki, K., 2006. Effect
684 of high iron concentrations on iron uptake and growth of a coastal diatom *Chaetoceros*
685 *sociale*. Aquat. Microb. Ecol. 43, 177–191. doi:10.3354/ame043177.
686 Jickells, T.D., An, Z.S., Andersen, K.K., Baker, A.R., Bergametti, G., Brooks, G., Cao, J.J.,
687 Boyd, P.W., Duce, R.A., Hunter, K.A., Kawahata, H., Kubilay, N., laRoche, J., Liss,
688 P.S., Mahowald, N., Prospero, J.M., Ridgwell A.J., Tegen, I., Torres, R., 2005. Global

689 iron connections between desert dust, ocean biogeochemistry, and climate. Science 308,
690 67–71. doi:10.1126/science.1105959.
691 Johnson, K.S., Chavez, F.P., Friederich, G.E., 1999. Continental-shelf sediment as a primary
692 source of iron for coastal phytoplankton. Nature 398, 697–700.
693 Johnson, K.S., Miller, L.A., Sutherland, N.E., Wong, C.S., 2005. Iron transport by mesoscale
694 Haida eddies in the Gulf of Alaska. Deep-Sea Res. II 52, 933–953.
695 doi:10.1016/j.dsr2.2004.08.017.
696 Kitayama, S., Kuma, K., Manabe, E., Sugie, K., Takata, H., Isoda, Y., Toya, K., Saitoh, S.,
697 Takagi, S., Kamei, Y., Sakaoka, K., 2009. Controls on iron distributions in the deep
698 water column of the North Pacific Ocean: Iron(III) hydroxide solubility and marine
699 humic-type dissolved organic matter. J. Geophys. Res. 114, C08019,
700 doi:10.1029/2008JC004754.
701 Komuro, C., Narita, H., Imai, K., Nojiri, Y., Jordan, R.W., 2005. Microplankton assemblage
702 at Station KNOT in the subarctic western Pacific, 1999–2000. Deep-Sea Res. II 52,
703 2206–2217. doi:10.1016/j.dsr2.2005.08.006.
704 Kuma, K., Matsunaga, K., 1995. Availability of colloidal ferric oxides to coastal marine
705 phytoplankton. Mar. Biol. 122, 1–11.
706 Kuma, K., Nishioka, J., Matsunaga, K., 1996. Controls on iron(III) hydroxide solubility in
707 seawater: The influence of pH and natural organic chelators. Limnol. Oceanogr. 41,
708 396–407.
709 Kuma, K., Tanaka, J., Matsunaga, K., Matsunaga, K., 2000. Effect of hydroxamate
710 ferrisiderophore complex (ferrichrome) on iron uptake and growth of a coastal marine
711 diatom *Chaetoceros sociale*. Limnol. Oceanogr. 45, 1234–1244.
712 Kustka, A.B., Allen, A.E., Morel, F.M.M., 2007. Sequence analysis and transcriptional
713 regulation of iron acquisition genes in two marine diatoms. J. Phycol. 43, 715–729.
714 doi:10.1111/j.1529-8817.2007.00359.x.
715 Landing, W.M., Bruland, K.W., 1987. The contrasting biogeochemistry of iron and
716 manganese in the Pacific Ocean. Geochim. Cosmochim. Acta 51, 29–43.

Lohan, M. C., Bruland, K. M., 2006. Importance of vertical mixing for additional source of nitrate and iron to surface waters of the Columbia River plume: Implications for biology. Mar. Chem. 98, 260–273.

Maldonado, M.T., Price, N.M., 1999. Utilization of iron bound to strong organic ligands by plankton communities in the subarctic Pacific Ocean. Deep-Sea Res. II 46, 2447–2473.

Maldonado, M.T., Price, N.M., 2001. Reduction and transport of organically bound iron by *Thalassiosira oceanica* (Bacillariophyceae). J. Phycol. 37, 298–309.

Maranger, R., Bird, D.F., Price, N.M., 1998. Iron acquisition by photosynthetic marine phytoplankton from ingested bacteria. Nature 396, 248–251.

Marchetti, A., Maldonado, M.T., Lane, E.S., Harrison, P.J., 2006. Iron requirements of the pennate diatom *Pseudo-nitzschia*: Comparison of oceanic (HNLC) and coastal species. Limnol. Oceanogr. 51, 2092–2101.

Marchetti, A., Parker, M.S., Moccia, L.P., Lin, E.O., Arrieta, A.L., Ribalet, F., Murphy, M.E.P., Maldonado, M.T., Armbrust, E.V., 2009. Ferritin is used for iron storage in bloom-forming marine pennate diatoms. Nature 457, 467–470. doi:10.1038/nature07539.

Martin, J.H., Gordon, R.M., Fitzwater, S., Broenkow, W.W., 1989. VERTEX: phytoplankton/iron studies in the Gulf of Alaska. Deep-Sea Res. 36, 649–680.

Matsuda, J., Mitsudera, H., Nakamura, T., Uchimoto, K., Nakanowatari, T., Ebuchi, N., 2009. Wind and buoyancy driven intermediate-layer overturning in the Sea of Okhotsk. Deep-Sea Res. I 56, 1401–1418. doi:10.1016/j.dsr.2009.04.014.

Mayer, L. M., Schick, L. L., Hardy, K. R., Estapa, M. L., 2009. Photodissolution and other photochemical changes upon irradiation of algal detritus. Limnol. Oceanogr. 54, 1688–1698.

McQuoid, M.R., Hobson, L.A., 1996. Diatom resting stages. J. Phycol. 32, 889–902.

Misumi, K., Tsumune, D., Yoshida, Y., Uchimoto, K., Nakamura, T., Nishioka, J., Mitsudera, H., Bryan, F.O., Lindsay, K., Moor, J.K., and Doney, S.C., 2011. Mechanisms controlling dissolved iron distribution in the North Pacific: A model study. J. Geophys. Res. 116, G03005. doi:10.1029/2010JG001541.

Moore, J.K., Braucher, O., 2008. Sedimentary and mineral dust sources of dissolved iron to the world ocean. Biogeosciences 5, 631–656.

747 Morel, F.M.M., Rueter, J.G., Anderson, D.M., Guillard, R.R.L., 1979. AQUIL: A chemically
748 defined phytoplankton culture medium for trace metal studies. J. Phycol. 15, 135–141.
749 Morel, F.M.M., Kustka, A.B., Shaked, Y., 2008. The role of unchelated Fe in the iron
750 nutrition of phytoplankton. Limnol. Oceanogr. 53, 400–404.
751 Nakamura, T., Awaji, T., 2004. Tidally induced diapycnal mixing in the Kuril Straits and its
752 role in water transformation and transport: A three-dimensional nonhydrostatic model
753 experiments. J. Geophys. Res. 109, C09S07, doi:10.1029/2003JC001850.
754 Nakatsuka, T., Toda, M., Kawamura, K., Wakatsuchi, M., 2004. Dissolved and particulate
755 organic carbon in the Sea of Okhotsk: Transport from continental shelf to ocean interior.
756 J. Geophys. Res. 109, C09S14, doi:10.1029/2003JC001909.
757 Nakayama, Y., Kuma, K., Fujita, S., Sugie, K., Ikeda, T., 2010. Temporal variability and
758 bioavailability of iron and other nutrients during the spring phytoplankton bloom in the
759 Oyashio region. Deep-Sea Res. II 57, 1618–1629. doi:10.1016/j.dsr2.2010.03.006.
760 Nishioka, J., Takeda, S., 2000. Change in the concentrations of iron in different size fractions
761 during growth of the oceanic diatom *Chaetoceros* sp.: importance of small colloidal iron.
762 Mar. Biol. 137, 231–238. doi:10.1007/s002270000347.
763 Nishioka, J., Takeda, S., Wong, C.S., 2001. Change in the concentrations of iron in different
764 size fractions during a phytoplankton bloom in controlled ecosystem enclosures. J. Exp.
765 Mar. Biol. Ecol. 258, 237–255. doi:10.1016/S0022-0981(01)00219-2.
766 Nishioka, J., Takeda, S., Kudo, I., Tsumune, D., Yoshimura, T., Kuma, K., Tsuda, A., 2003.
767 Size-fractionated iron distributions and iron-limitation processes in the subarctic NW
768 Pacific. Geophys. Res. Lett. 30, 14, 1730, doi:10.1029/2002GL016853.
769 Nishioka, J., Ono, T., Saito, H., Nakatsuka, T., Takeda, S., Yoshimura, T., Suzuki, K., Kuma,
770 K., Nakabayashi, S., Tsumune, D., Mitsudera, H., Johnson, W.K., Tsuda, A., 2007. Iron
771 supply to the western subarctic Pacific: Importance of iron export from the Sea of
772 Okhotsk. J. Geophys. Res. 112, C10012, doi:10.1029/2006JC004055.
773 Nishioka, J., Ono, T., Saito, H., Sakaoka, K., Yoshimura, T., 2011. The annual cycle of
774 surface iron and the source of iron supporting the spring diatom bloom in the Oyashio
775 region, western subarctic Pacific. J. Geophys. Res. 116, C02021,
776 doi:10.1029/2010JC006321.

777 Obata, H., Karatani, H., Nakayama, E., 1993. Automated determination of iron in seawater by
778 chelating resin concentration and chemiluminescence detection. Anal. Chem. 65,
779 1524–1528.
780 Passow, U., 2002. Transparent exopolymer particles (TEP) in aquatic environments. Prog.
781 Oceanogr. 55, 287–333. doi:10.1016/S0079-6611(02)00138-6.
782 Paytan, A., Mackey, K.R.M., Chen, Y., Lima, I.D., Doney, S.C., Mahowald, N., Labiosa, R.,
783 Post, A.F., 2009. Toxicity of atmospheric aerosols on marine phytoplankton. Proc. Natl.
784 Acad. Sci. U.S.A. 106, 4601–4605. doi:10.1073/pnas.0811486106.
785 Poorvin, L., Rinta-Kanto, J.M., Hutchins, D.A., Wilhelm, S.W., 2004. Viral release of iron
786 and its bioavailability to marine plankton. Limnol. Oceanogr. 49, 1734–1741.
787 Price, N.M., Ahner, B.A., Morel, F.M., 1994. The equatorial Pacific Ocean:
788 Grazer-controlled phytoplankton populations in an iron-limited ecosystem. Limnol.
789 Oceanogr. 39, 520–534.
790 Price, N.M., 2005. The elemental stoichiometry and composition of an iron-limited diatom.
791 Limnol. Oceanogr. 50, 1159–1171.
792 Raven, J.A., 1988. The iron and molybdenum use efficiencies of plant growth with different
793 energy, carbon and nitrogen sources. New Phytol. 109, 279–287.
794 Raven, J.A., Evans, M.C.W., Korb, R.E., 1999. The role of trace metals in photosynthetic
795 electron transport in O_2-evolving organisms. Photosynthesis Res. 60, 111–149.
796 Redfield, A.C., Ketchum, B.H., Richards, F.A., 1963. The influence of organisms on the
797 composition of seawater. In: Hill, M.N. (Ed.), The Sea. Vol. 2. Wiley, New York, pp.
798 26–77.
799 Rue, E.L., Bruland, K.W., 1995. Complexation of iron(III) by natural organic ligands in the
800 Central North Pacific as determined by a new competitive ligand equibration / adsorptive
801 cathodic stripping voltammetric method. Mar. Chem. 50, 117–138.
802 Shaked, Y., Kustka, A.B., Morel, F.M.M., 2005. A general kinetic model for iron acquisition
803 by eukaryotic phytoplankton. Limnol. Oceanogr. 50, 872–882.

804 Shcherbina, A.Y., Talley, L.D., Rudnick, D.L., 2004. Dense water formation on the
805 northwestern shelf of the Okhotsk Sea: 1. Direct observations of brine rejection. J.
806 Geophys. Res. 109, C09S08, doi:10.1029/2003JC002196.
807 Shigemitsu, M., Okunishi, T., Nishioka, J., Sumata, H., Hashioka, T., Aita, M.N., Smith, S.L.,
808 Yoshie, N., Okada, N., Yamanaka, Y., 2012. Development of a one-dimensional
809 ecosystem model including the iron cycle applied to the Oyashio region, western
810 subarctic Pacific. J. Geophys. Res. 117, C06021, doi:10.1029/2011JC007689.
811 Strzepek, R.F., Harrison, P.J., 2004. Photosynthetic architecture differs in coastal and oceanic
812 diatoms. Nature 431, 689–692.
813 Strzepek, R.F., Maldonado, M.T., Hunter, K.A., Frew, R.D., Boyd, P.W., 2011. Adaptive
814 strategies by Southern Ocean phytoplankton to less iron limitation: Uptake of
815 organically complexed iron and reduced cellular iron requrements. Limnol. Oceanogr. 56,
816 1983–2002. doi:10.4319/lo.2011.56.6.1983.
817 Stumm, W., Morgan, J.J., 1996. Aquatic Chemistry, 3rd ed. Wiley Interscience, New York.
818 Sugie, K., Yoshimura, T., in press. Effects of pCO_2 and iron on the elemental composition
819 and cell geometry of the marine diatom *Pseudo-nitzschia pseudodelicatissima*
820 (Bacillariophyceae). J. Phycol.
821 Sugie, K., Kuma, K., Fujita, S., Nakayama, Y., Ikeda, T., 2010a. Nutrient and diatom
822 dynamics during late winter and spring in the Oyashio region of the western subarctic
823 Pacific Ocean. Deep-Sea Res. II 57, 1630–1642. doi:10.1016/j.dsr2.2010.03.007.
824 Sugie, K., Kuma, K., Fujita, S., Ikeda, T., 2010b. Increase in Si:N drawdown ratio due to
825 resting spore formation by spring bloom-forming diatoms under Fe- and N-limited
826 conditions in the Oyashio region. J. Exp. Mar. Biol. Ecol. 382, 108–116.
827 doi:10.1016/j.jembe.2009.11.001.
828 Sugie, K., Kuma, K., Fujita, S., Ushizaka, S., Suzuki, K., Ikeda, T., 2011. Importance of
829 intracellular Fe pools on growth of marine diatoms by using unialgal cultures and the
830 Oyashio region phytoplankton community during spring. J. Oceanogr. 67, 183–196.
831 doi:10.1007/s10872-011-0017-4.

832 Sunda, W.G., Huntsman, S.A., 1995. Iron uptake and growth limitation in oceanic and coastal
833 phytoplankton. Mar. Chem. 50, 189–206.
834 Suzuki, K., Minami, C., Liu, H., Saino, T., 2002. Temporal and spatial patterns of
835 chemotaxonomic algal pigments in the subarctic Pacific and the Bering Sea during the
836 early summer of 1999. Deep-Sea Res. II 49, 5685–5704.
837 Suzuki, R., Ishimaru, T., 1990. An improved method for the determination of phytoplankton
838 chlorophyll using N, N-dimethylformamide. J. Oceanogr. Soc. Jpn. 46, 190–194.
839 Throndsen, J., 1978. Centrifugation. In: Sourina, A., (Ed.), Phytoplankton manual. UNESCO,
840 Paris, pp. 98–103.
841 Timmermans, K.R., van der Wagt, B., Veldhuis, M.J.W., Maatman, A., de Baar, H.J.W., 2005.
842 Physiological responses of three species of marine pico-photoplankton to ammonium,
843 phosphate, iron and light limitation. J. Sea Res. 53, 109–120.
844 doi:10.1016/j.seares.2004.05.003.
845 Tortell, P.D., Maldonado, M.T., Price, N.M., 1996. The role of heterotrophic bacteria in
846 iron-limited ocean ecosystems. Nature 383, 330–332.
847 Twining, B.S., Baines, S.B., Fisher, N.S., Landry, M.R., 2004. Cellular iron contents of
848 plankton during the Southern Ocean Iron Experiment (SOFeX). Deep-Sea Res. I 51,
849 1827–1850. doi:10.1016/j.dsr.2004.08.007.
850 Wells, M.L., 1999. Manipulating iron availability in nearshore waters. Limnol. Oceanogr. 44,
851 1002–1008.
852 Wells, M.L., 2002. Marine colloids and trace metals. In: Hansell, D.A. and Carlson, C.A.
853 (Eds.), Biogeochemistry of marine dissolved organic matter. Elsevier Science, U.S.A., p.
854 367–404.
855 Welschmeyer, N.A., 1994. Fluorometric analysis of chlorophyll *a* in the present of
856 chlorophyll *b* and pheopigments. Limnol. Oceanogr. 39, 1985–1992.
857 Yamamoto, M., Tanaka, N., Tsunogai, S., 2001. Okhotsk Sea intermediate water formation
858 deduced from oxygen isotope systematics. J. Geophys. Res. 106, 31075–31084.
859 Yasuda, I., Kouketsu, S., Katsumata, K., Ohiwa, M., Kawasaki, Y., Kusaka, A., 2002.
860 Influence of Okhotsk Sea intermediate water on the Oyashio and North Pacific
861 Intermediate Water. J. Geophys. Res. 107, C12, 3237, doi:10.1029/2001JC001037.

862 Yoshida, M., Kuma, K., Iwade, S., Isoda, Y., Takata, H., Yamada, M., 2006. Effect of aging
863 time on the availability of freshly precipitated ferric hydroxide to coastal marine diatoms.
864 Mar. Biol. 149, 379–392. doi:10.1007/s00227-005-0187-y.
865 Yoshimura, T., Nishioka, J., Nakatsuka, T., 2010. Iron nutritional status of the phytoplankton
866 assemblage in the Okhotsk Sea during summer. Deep-Sea Res. I 57, 1454–1464.
867 doi:10.1016/j.dsr.2010.08.003.
868
869
870 Table and figure captions
871 Table 1. Experimental design of six treatments to test the bioavailability of particulate Fe
872 collected from dense shelf water (SPM_{DSW}) for the Fe-limited phytoplankton community.
873 Symbols of plus and minus represent the factors added or not added, respectively. *: Not
874 an extra addition, but natural SPM and phytoplankton are present in the DSW_{raw}
875 treatment.
876 Table 2. Phytoplankton abundance ($\times 10^3$ cells L^{-1}) and apparent growth rate (day 0 to 5) of
877 centric and pennate diatoms during the SPM_{DSW} addition experiment.
878 Table 3. Nutrient drawdown (in μmol L^{-1}) and its ratios during 5 days of the SPM_{DSW}
879 addition experiment. Data represent mean ± 1SD of triplicate incubation bottles. *:
880 Nutrient concentrations and drawdown ratios were offset by subtracting the value
881 dissociated from the SPM_{DSW} measured in the SPM_{DSW}−Phy treatment.
882 Table 4. Phytoplankton abundance ($\times 10^3$ cells L^{-1}) and apparent growth rate (day 0 to 5) of
883 centric and pennate diatoms and flagellates during the surface water incubations.
884 Table 5. Published elemental composition of the phytoplankton and seston under Fe-limited
885 conditions. The reported values of Fe-starved phytoplankton, cultivated with strong
886 chelator such as desferrioxamine B were excluded. Values with * indicate that
887 extracellularly absorbed iron was not eliminated, whereas the other values represent
888 intracellular elemental compositions. n.d.: no data. †: Fe:Chl-a values with no Chl-a:C
889 measurement were estimated using other reported Chl-a:C values (0.08–0.38 g:mol).

Figure 1. Sampling locations around the Sea of Okhotsk. The gray contours are shown at a 1000 m isobath interval. Abbreviations; DSW: dense shelf water, Ok: Okhotsk, BS: Bussol' Strait, and Oy: Oyashio.

Figure 2. Vertical profiles of (a) temperature, (b) salinity (c) sigma-*t* and (d) beam transmission at the beginning of the SPM_{DSW} addition experiment at Stn. DSW.

Figure 3. (a) Temporal change in chlorophyll-*a* concentrations examining Fe bioavailability in the suspended particulate matter collected from DSW (SPM_{DSW}) at Stn. DSW. Data represent mean ± 1SD for triplicate or mean ± range for duplicate analysis. The error bars are hidden when smaller than the symbols. (b) Specific growth rate for six treatments. Data represent mean ± 95% C.L. of regression (see method).

Figure 4. Vertical profiles of (a) temperature, (b) salinity and (c) sigma-*t* at the beginning of the surface phytoplankton incubation experiments.

Figure 5. Temporal changes in (a), (b) and (c) chlorophyll-*a* (Chl *a*), (d), (e) and (f) NO_3+NO_2, and (g), (h) and (i) $Si(OH)_4$ at station Oyashio (a, d and g), Bussol' Strait (b, e and h) and Okhotsk (c, f and i). Data represent mean ± 1SD for triplicate incubation bottles.

Figure 6. Diatom species composition and cell densities at the start of the surface phytoplankton incubation experiments at station Oyashio (Oy), Bussol' Strait (BS) and Okhotsk (Ok).

Figure 7. Comparing phytoplankton response during the surface phytoplankton incubation experiments in terms of (a) the relative growth rate in the unamended control to the Fe-added treatment ($\mu_{control}/\mu_{Fe\text{-}added}$), (b) difference in the increased Chl-*a* between the control and the DFB treatment ([ΔChl-*a*]), (c) difference in the NO_3+NO_2 drawdown between the control and the DFB treatment ([ΔNO_3+NO_2]), and (d) difference in ΔNH_4^+ drawdown between the control and the DFB treatment ([ΔNH_4^+]). Data represents mean ± 1SD for triplicate incubation bottles.

Table 1. Experimental design of six treatments to test the bioavailability of particulate Fe collected from dense shelf water (SPM_{DSW}) for the Fe-limited phytoplankton community. Symbols of plus and minus represent the factors added or not added, respectively. *: Not an extra addition, but natural SPM and phytoplankton are present in the DSW_{raw} treatment.

Treatment	Phytoplankton	Fe	SPM_{DSW}	DFB
Control	+	−	−	−
Fe	+	+	−	−
DFB	+	−	−	+
SPM_{DSW}	+	−	+	−
SPM_{DSW}−Phy	−	−	+	−
DSW_{raw}	−*	−	−*	−

Table 2. Phytoplankton abundance ($\times 10^3$ cells L^{-1}) and apparent growth rate (day 0 to 5) during the SPM_{DSW} addition experiment.

Treatments	Abundance at day 0		Abundance at day 5		Growth rate (d^{-1})	
	Centric	Pennate	Centric	Pennate	Centric	Pennate
Controls	2.6	1350	39	21300	0.54	0.55
Fe	2.6	1350	40	41400	0.54	0.68
DFB	2.6	1350	44	1700	0.56	0.05
SPM_{DSW}	28	1410	173	120000	0.84	0.90
SPM_{DSW}−Phy	28	56	84	39	0.22	−0.07
DSW_{raw}	0.32	0.30	52	28	1.0	0.90

Table 3. Nutrient drawdown (in μmol L^{-1}) and its ratios during 5 day incubation experiment. Data represent mean ± 1SD of triplicate incubation bottles.

Treatment	ΔDIN	ΔP	ΔSi	ΔSi: ΔN	ΔN: ΔP	ΔSi: ΔP
Control	14.4 ± 0.38	0.95 ± 0.16	4.00 ± 1.09	0.28 ± 0.07	15.7 ± 2.94	4.45 ± 1.68
Fe	21.7 ± 1.04	1.48 ± 0.04	7.55 ± 0.84	0.35 ± 0.02	14.7 ± 0.48	5.10 ± 0.49
DFB	6.95 ± 0.61	0.69 ± 0.09	−1.15 ± 1.20	−0.18 ± 0.18	10.1 ± 0.48	−1.89 ± 1.82
SPM_{DSW}	38.2 ± 1.05*	1.95 ± 0.06*	28.1 ± 1.16*	0.74 ± 0.03*	19.6 ± 0.71*	14.4 ± 0.20*
SPM_{DSW}−Phy	−1.92 ± 1.60	−0.17 ± 0.22	−10.9 ± 3.95	9.88 ± 6.36	3.59 ± 24.1	−93.4 ± 313
DSW_{raw}	1.18 ± 0.85	0.16 ± 0.13	1.29 ± 2.37	−0.76 ± 2.56	9.42 ± 2.37	−13.2 ± 25.9

*: Nutrient concentrations and drawdown ratios were offset by subtracting the value dissociated from the SPM_{DSW} in the SPM_{DSW}−Phy treatment.

Table 4. Phytoplankton abundance ($\times 10^3$ cells L^{-1}) and apparent growth rate (day 0 to 5) during the surface water incubations.

Station		Initial	Abundance at day 5			Growth rate (d^{-1})		
			Cont.	Fe	DFB	Cont.	Fe	DFB
Oy	Centric diatoms	0.40	24.8	23.2	6.46	0.83	0.81	0.55
	Pennate diatoms	1.67	434	814	136	1.11	1.24	0.88
	Flagellates	89.7	573	907	123	0.83	0.92	0.52
BS	Centric diatoms	1.18	119	124	25.2	0.92	0.93	0.61
	Pennate diatoms	3.90	557	661	107	0.99	1.02	0.66
	Flagellates	62.6	2926	4514	705	1.23	1.32	0.94
Ok	Centric diatoms	1.44	45.7	316	34.1	0.69	1.08	0.63
	Pennate diatoms	4.16	2080	3330	596	1.24	1.34	0.99
	Flagellates	17.1	9760	11600	358	1.27	1.30	0.61

Table 5. Published elemental composition of the phytoplankton and seston under Fe-limited conditions. The reported values of Fe-starved phytoplankton, cultivated with strong chelator such as desferrioxamine B were excluded. Values with * indicate that extracellularly absorbed iron was not eliminated, whereas the other values represent intracellular elemental compositions. n.d.: no data. †: Fe:Chl-*a* values with no Chl-*a*:C measurement were estimated using other reported Chl-*a*:C values (0.08–0.38 g:mol).

Data source	Fe:C (μmol:mol)	Chl-*a*:C (g:mol)	Fe:Chl-*a* (μmol:g)	Reference
Unialgal culture				
Diatom				
Eucampia antarctica (oceanic)	1.8	n.d.	4.7–23†	Strzepek et al., 2011
Fragilariopsis kerguelensis (oceanic)	4.2	n.d.	10–53†	Strzepek et al., 2011
Probosira inermis (oceanic)	4.5	n.d.	12–56†	Strzepek et al., 2011
Pseudo-nitzschia spp. (oceanic)	2.8–3.7	n.d.	10–35†	Marchetti et al., 2006
Pseudo-nitzschia spp. (coastal)	5.2–11	n.d.	29–65†	Marchetti et al., 2006
Thalassiosira weissflogii (coastal)	10.6	0.08	23	Price, 2005
T. weissflogii (coastal)	13–22	0.11–0.31	63–115	Sunda and Huntsman, 1995
Thalassiosira pseudonana (coastal)	13–25	0.12–0.21	82–123	Sunda and Huntsman, 1995
Thalassiosira oceanica (oceanic)	2.5–7.1	0.17–0.32	11–28	Sunda and Huntsman, 1995
Others				
Emiliania huxleyi (oceanic)	4.1–6.0	0.16–0.38	16–29	Sunda and Huntsman, 1995
Pelagomonas calceolata (oceanic)	4.3–9.6	0.26–0.32	14–32	Sunda and Huntman, 1995
Phaeocystis antarctica (oceanic)	8.6	n.d.	23–108†	Strzepek et al., 2011
Prorocentrum minimum (coastal)	11–20	0.12–0.16	89–129	Sunda and Huntman, 1995
Natural particle				
Phytoplankton	6.0–8.7*	n.d.	23–75†	Twining et al., 2004
Seston	30*	n.d.	79–375†	Martin et al., 1989
Seston	3.7	n.d.	9.7–46†	Maldonado and Price, 1999

Figure 1

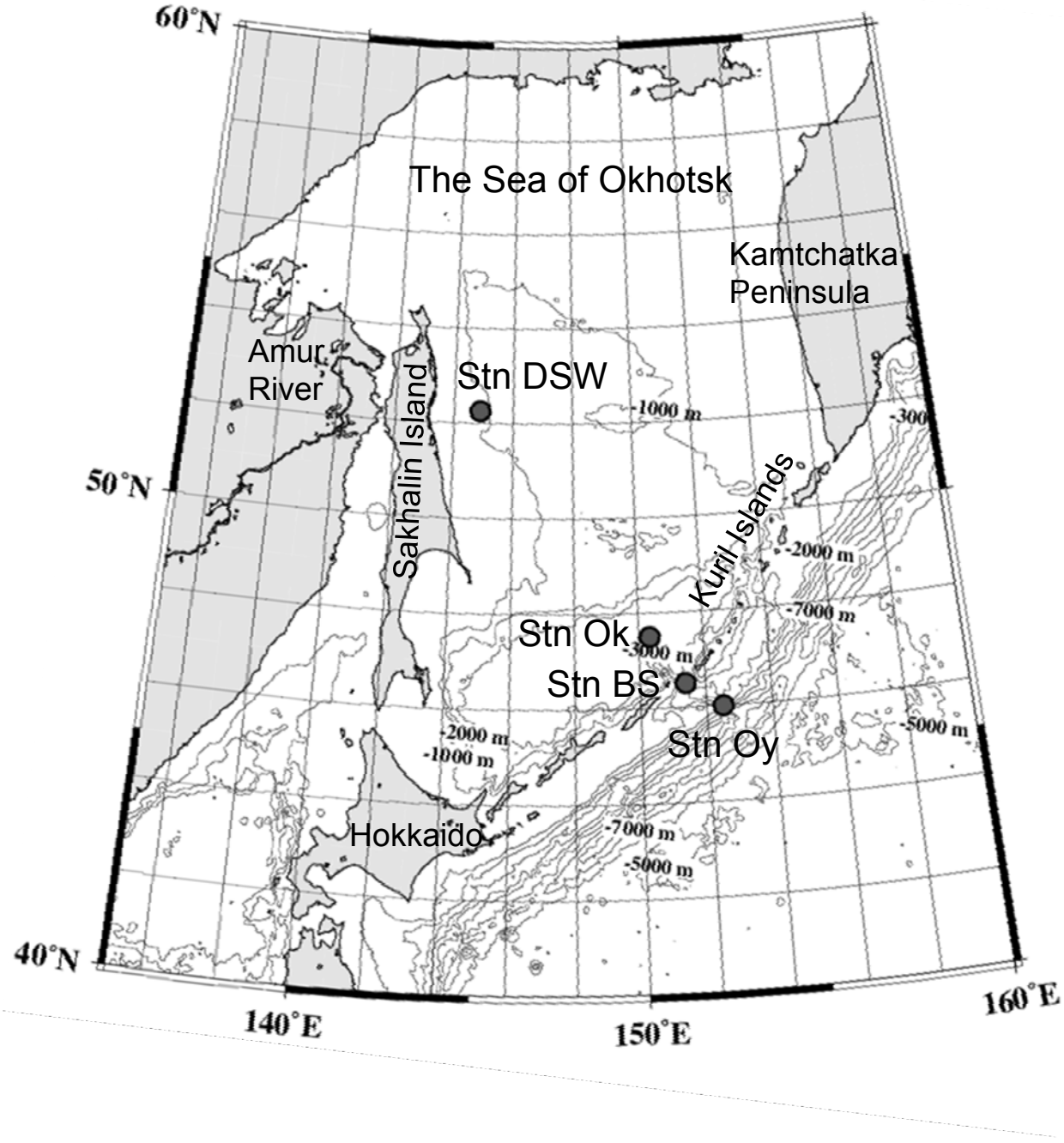
60°N
50°N
40°N
140°E
150°E
160°E
The Sea of Okhotsk
Kamtchatka Peninsula
Amur River
Sakhalin Island
Stn DSW
Kuril Islands
Stn Ok
Stn BS
Stn Oy
Hokkaido
-1000 m
-2000 m
-3000 m
-5000 m
-7000 m

Figure 2

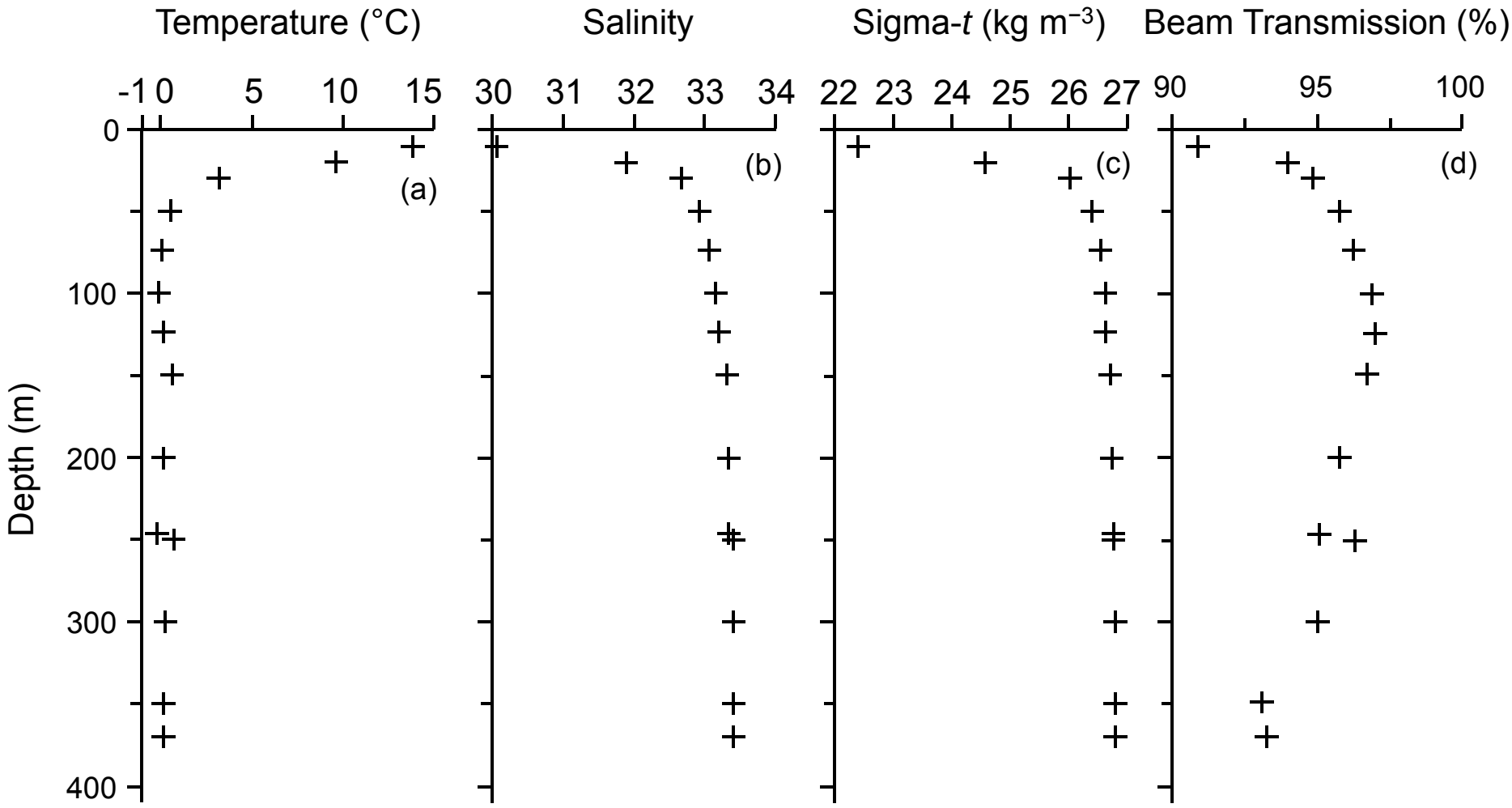
Temperature (°C)
Salinity
Sigma-t (kg m−3)
Beam Transmission (%)
-1 0 5 10 15
30 31 32 33 34
22 23 24 25 26 27
90 95 100
(a)
(b)
(c)
(d)
Depth (m)
0
100
200
300
400

Figure 3

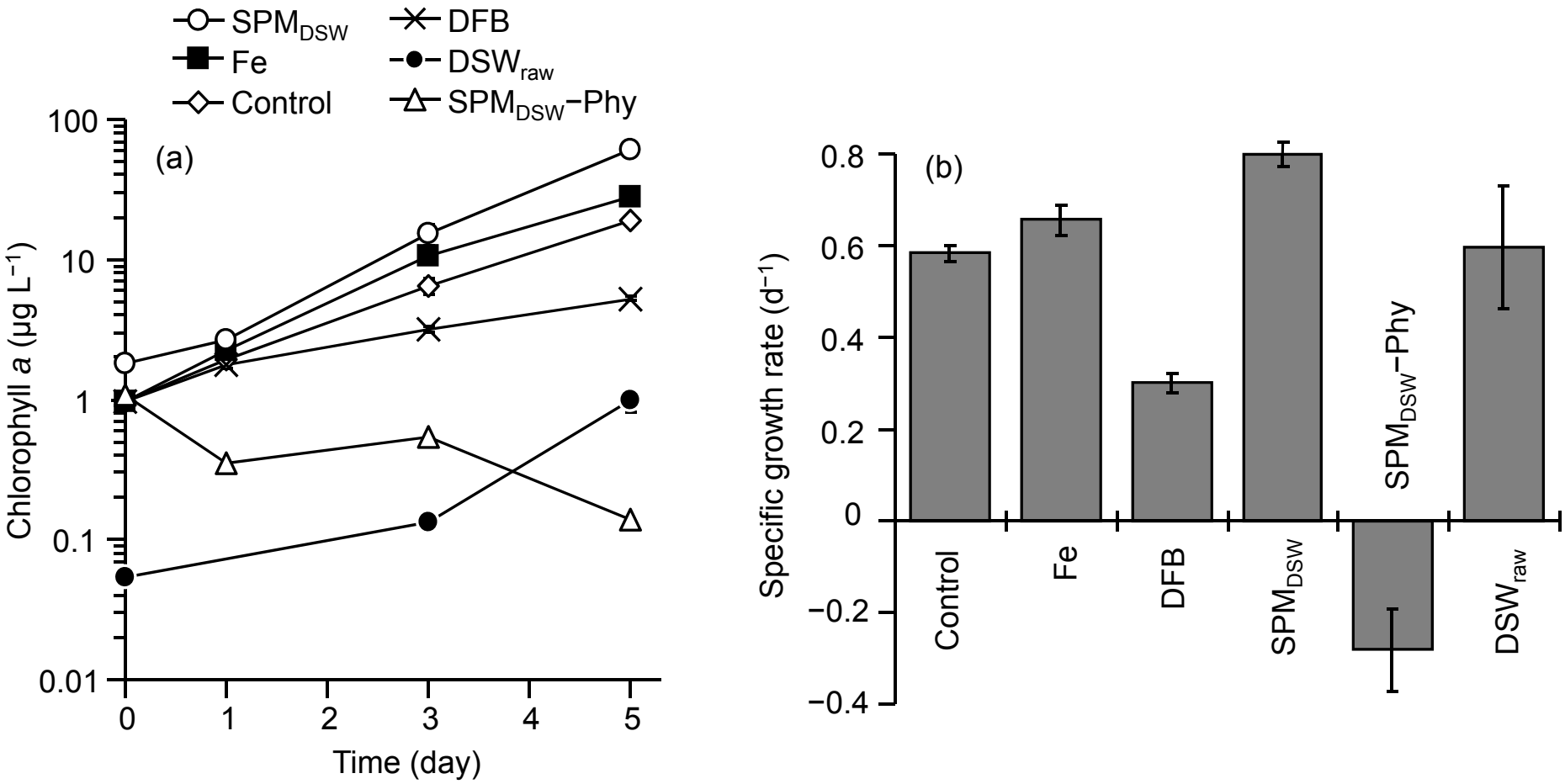
SPM$_{DSW}$
Fe
Control
DFB
DSW$_{raw}$
SPM$_{DSW}$−Phy
(a)
Chlorophyll a (μg L^{-1})
100
10
1
0.1
0.01
0
1
2
3
4
5
Time (day)
(b)
Specific growth rate (d^{-1})
0.8
0.6
0.4
0.2
0
−0.2
−0.4
Control
Fe
DFB
SPM$_{DSW}$
SPM$_{DSW}$−Phy
DSW$_{raw}$

Figure 4

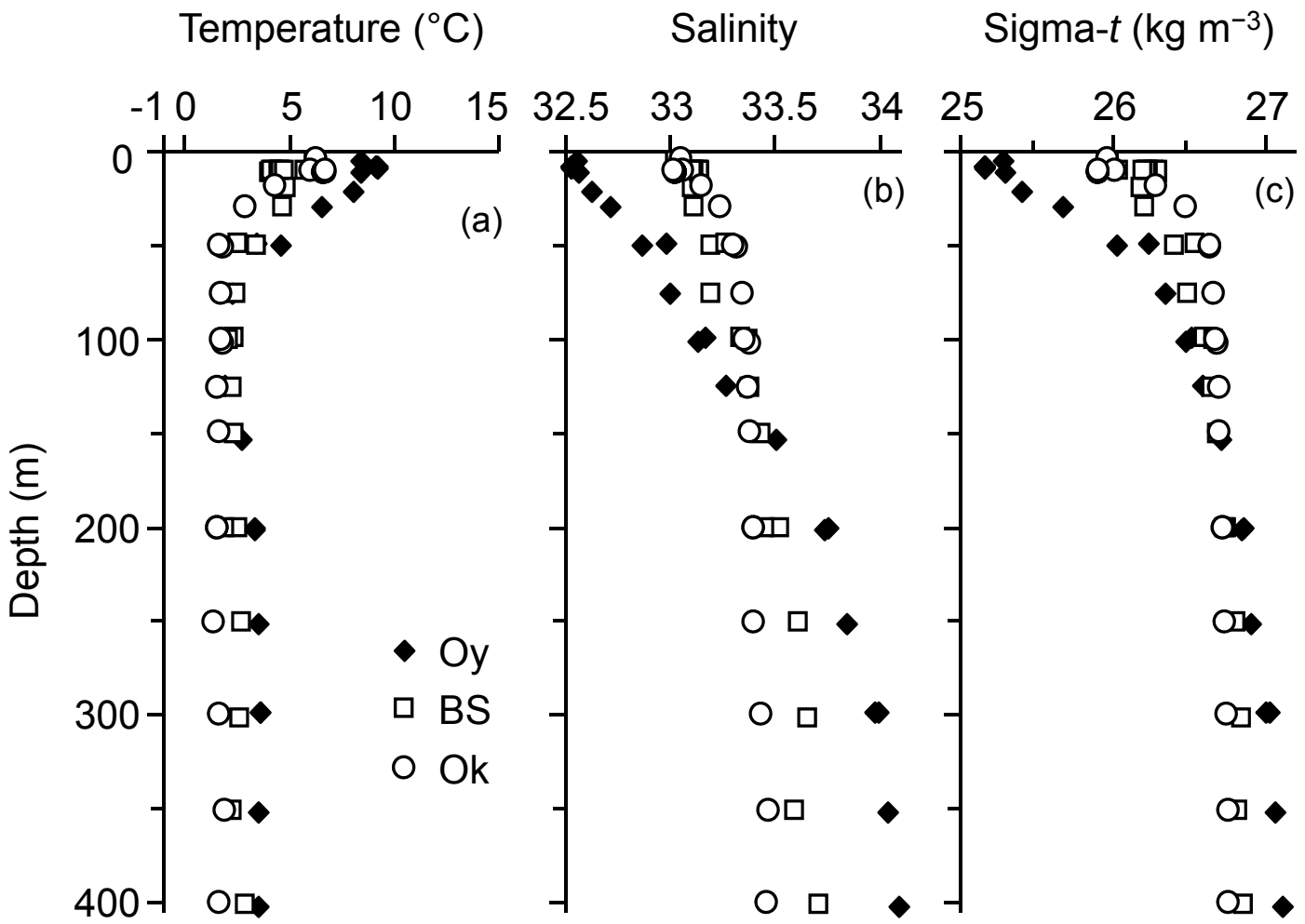
Temperature (°C)
Salinity
Sigma-t (kg m−3)
-1 0 5 10 15
32.5 33 33.5 34
25 26 27
0
100
200
300
400
Depth (m)
(a)
(b)
(c)
Oy
BS
Ok

Figure 5

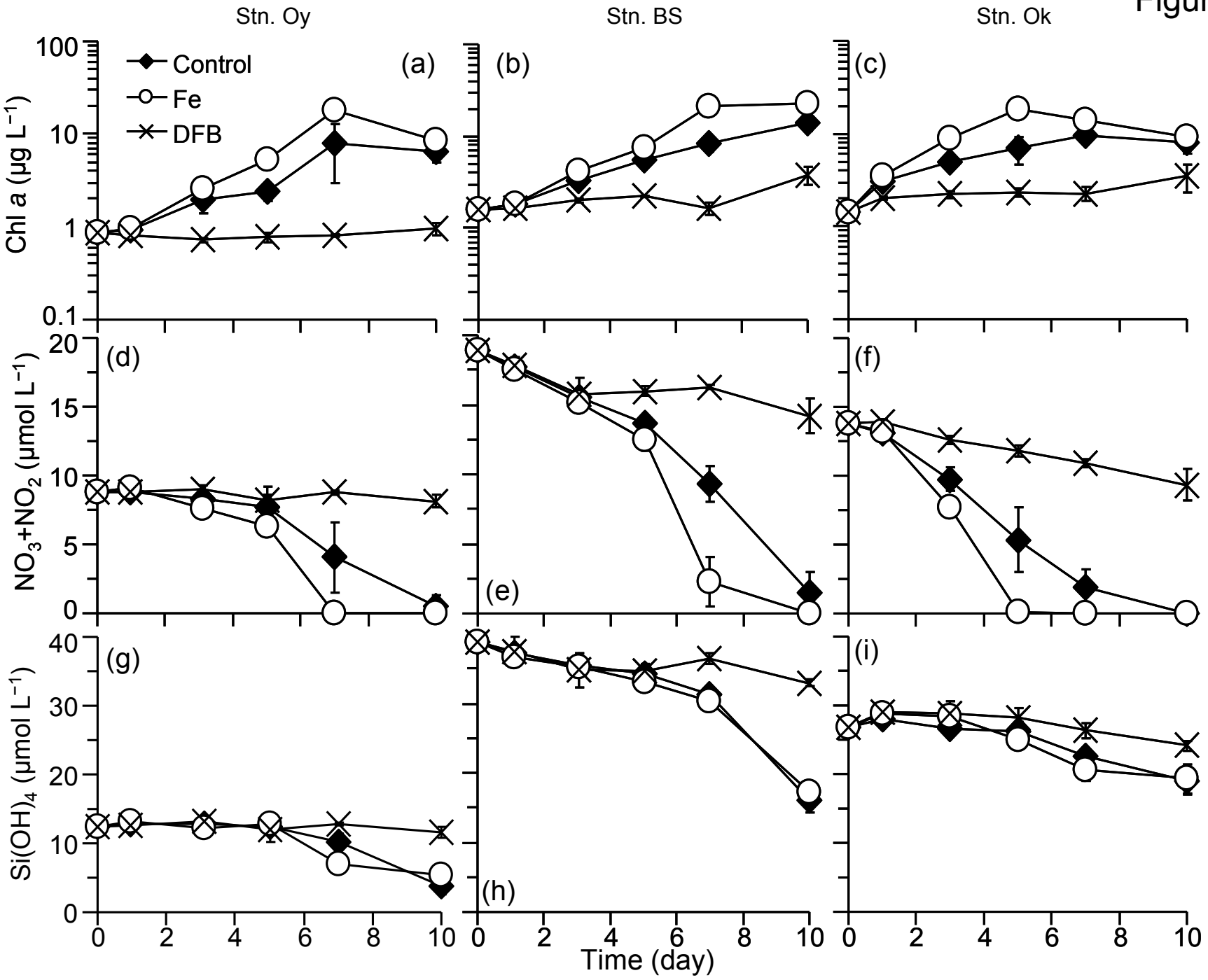
Stn. Oy
Stn. BS
Stn. Ok
Control
Fe
DFB
(a)
(b)
(c)
(d)
(e)
(f)
(g)
(h)
(i)
Chl a (μg L−1)
NO3+NO2 (μmol L−1)
Si(OH)4 (μmol L−1)
Time (day)
100
10
1
0.1
20
15
10
5
0
40
30
20
10
0
0
2
4
6
8
10

Figure 6

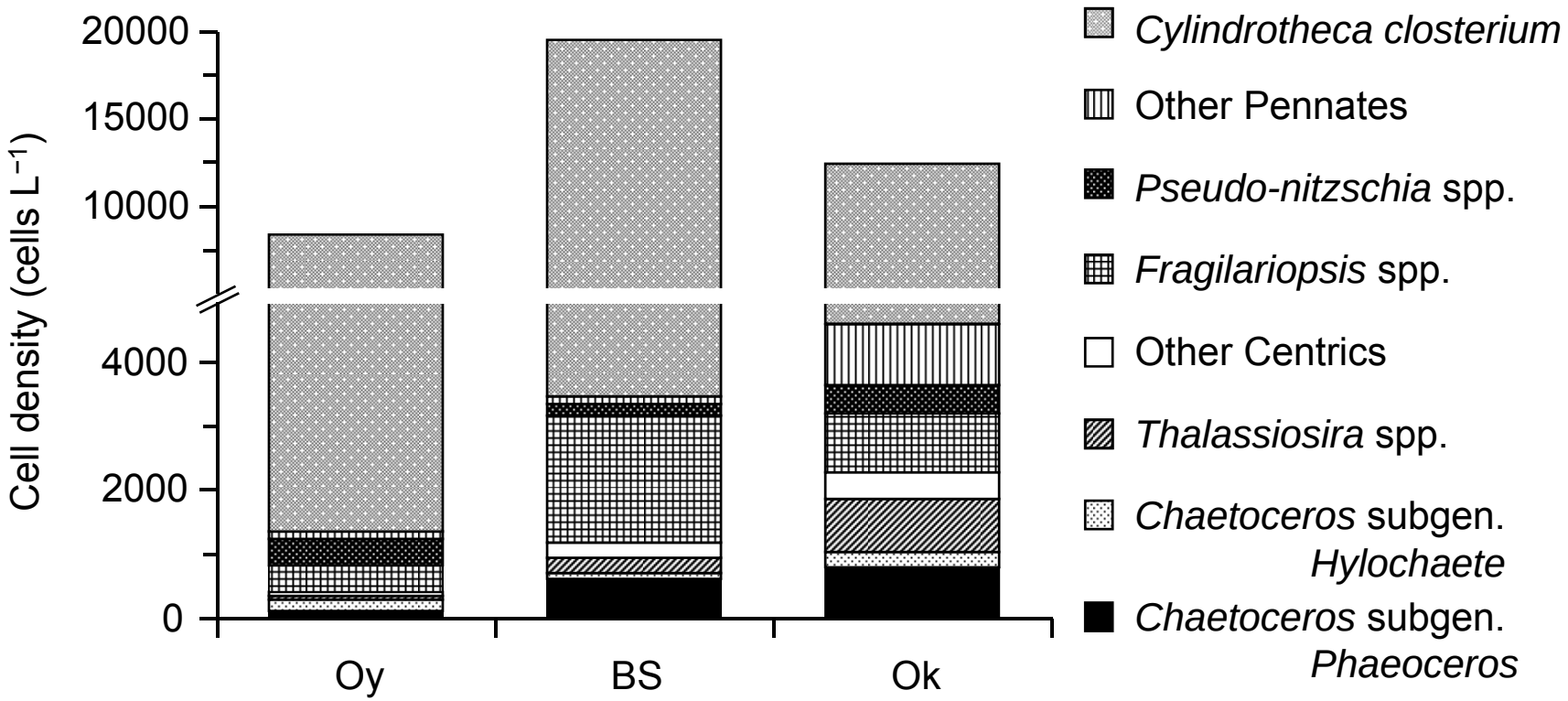
Cell density (cells L^{-1})
20000
15000
10000
4000
2000
0
Oy
BS
Ok
Cylindrotheca closterium
Other Pennates
Pseudo-nitzschia spp.
Fragilariopsis spp.
Other Centrics
Thalassiosira spp.
Chaetoceros subgen. *Hylochaete*
Chaetoceros subgen. *Phaeoceros*

Figure 7

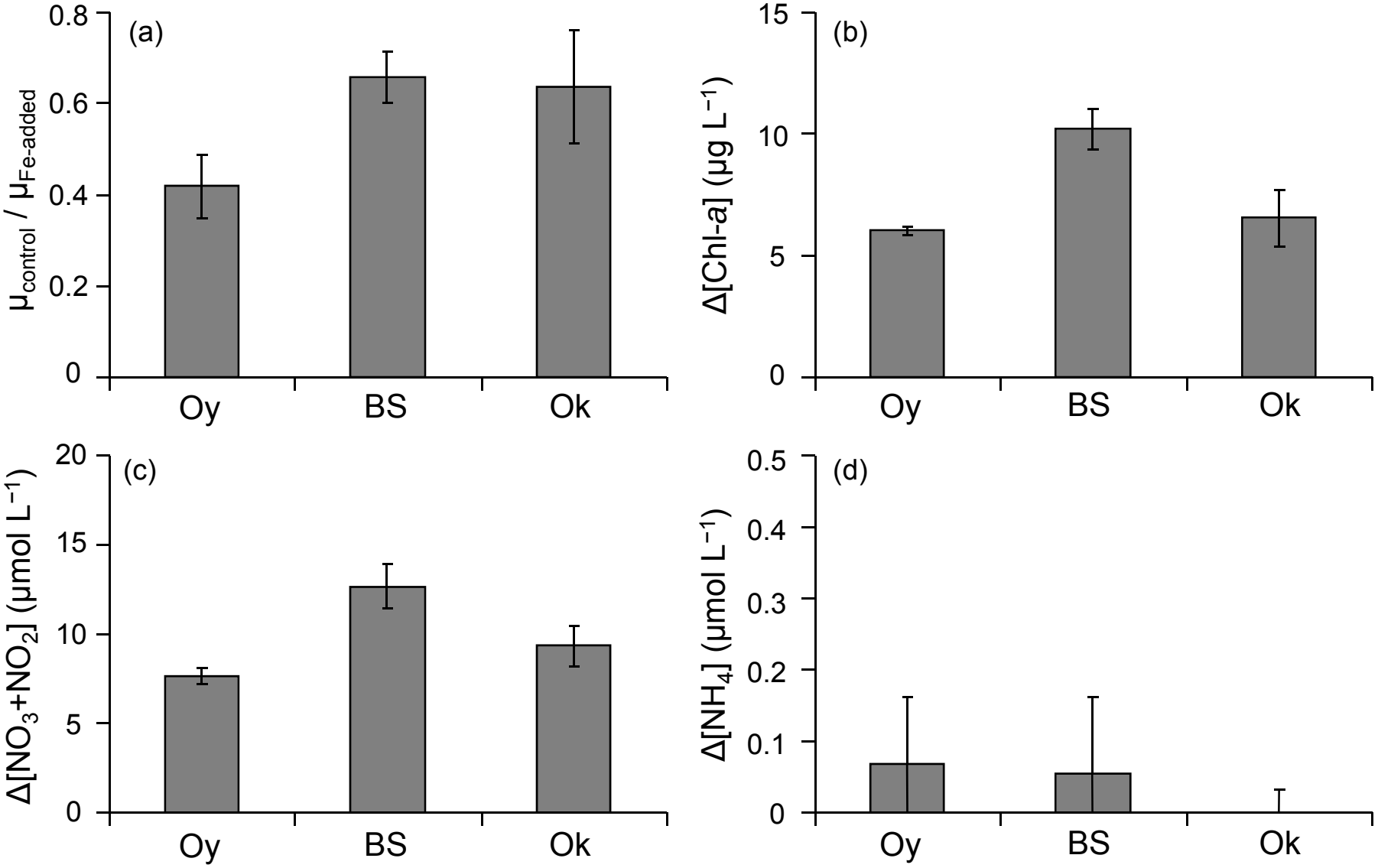
(a)
$\mu_{control}$ / $\mu_{Fe\text{-}added}$
0.8
0.6
0.4
0.2
0
Oy
BS
Ok
(b)
Δ[Chl-*a*] (μg L^{-1})
15
10
5
0
Oy
BS
Ok
(c)
Δ[NO_3+NO_2] (μmol L^{-1})
20
15
10
5
0
Oy
BS
Ok
(d)
Δ[NH_4] (μmol L^{-1})
0.5
0.4
0.3
0.2
0.1
0
Oy
BS
Ok